MODELLING GEOIDAL HEIGHTS IN THE GULF OF GUINEA USING JASON-2 SATELLITE ALTIMETRY DATA

BY

ABDULGANIYU ETUDAYE BELLO

DEPARTMENT OF GEOMATICS,

FACULTY OF ENVIRONMENTAL DESIGN,

AHMADU BELLO UNIVERSITY,

ZARIA, NIGERIA

OCTOBER, 2019

MODELLING GEOIDAL HEIGHTS IN THE GULF OF GUINEA USING JASON-2 SATELLITE ALTIMETRY DATA

BY

AbdulganiyuEtudaye BELLO,
B. TECH. (FUT MINNA) 2014
(P15EVGM8012)

A DISSERTATION SUBMITTED TO THE SCHOOL OF POSTGRADUATE STUDIES,
AHMADU BELLO UNIVERSITY, ZARIA
IN PARTIAL FULFILLMENT OF THE REQUIREMENTS FOR THE AWARD
OF MASTER OF SCIENCE DEGREE IN GEOMATICS

DEPARTMENT OF GEOMATICS,

FACULTY OF ENVIRONMENTAL DESIGN,

AHMADU BELLO UNIVERSITY,

ZARIA, NIGERIA

OCTOBER, 2019

DECLEARATION

I declare that the work in this project Dissertation entitled “MODELLING GEOIDAL HEIGHTS IN THE GULF OF GUINEA USING JASON-2 SATELLITE ALTIMETRY DATA”has beencarried out by me in the Department of Geomatics. The information derived from the literaturehas been duly acknowledged in the text and a list of references provided. No part of this Dissertationwas previously presented for another degree or diplomaat this or any other Institution..

AbdulganiyuEtudaye BELLO

Name	Signature	Date

CERTIFICATION

This project Dissertation entitled "MODELLING GEOIDAL HEIGHTS IN THE GULF OF GUINEA USING JASON-2 SATELLITE ALTIMETRY DATA" by AbdulganiyuEtudaye BELLO meets the regulations governing the award of the degree of MASTERS DEGREE IN GEOMATICS of the Ahmadu Bello University, and is approved for its contribution to knowledge and literary presentation.

Prof. L. M. Ojigi

(Chairman Supervisory Committee	(Signature)	(Date)

Dr. S. S.Garba

(Member Supervisory Committee)	(Signature)	(Date)

Dr. O. A. Isioye

(Head of Department)	(Signature)	(Date)

Prof. S.A. Abdullahi

(Dean, School of Postgraduate Studies)	(Signature)	(Date)

DEDICATION

I dedicate this Dissertation to my exalted mentor and beloved Muhammad bin Abdullahi bin Abdulmutallib for his love and concern on me. I ask almighty God to shower on him his mercy and favour (Amen).

ACKNOWLEDGEMENT

My profound gratitude to Almighty God who taught man what He does not know and for His grace on me for the successful accomplishment of my course work and this Dissertation.

My appreciation goes to my supervisors, Prof. L. M. Ojigiand Dr. S. Garbafor theirguidance, directives, useful information, valuable discussions suggestions corrections and facilitation of the appropriate data used for the project Dissertation.

Thanks to theformer Head of the department of Geomatics, Dr. T. T. Youngu and the present Head of the department, Dr. O. A. Isioye,for their efforts towards the success of the program. I do acknowledge the following lecturers;Dr, J. D. Dodo, Dr. S. S.Garba, Prof. A. A. Musa, Dr.T. O. Adewuyi, Prof. Kola Lawal of the Physics Department, all the academic, non-academic and technical staff of Geomatics Department inAhmadu Bello University, Zaria.

I express my gratitude to the AVISO, Eumetsat and NOAA Service Centre for providing a useful information license to access and use their altimetry data products.

I am thankful to all my colleagues in the class for their cooperation and support especially;Surv. SalisuBala and AwwalAbdulhameed. I acknowledge friends like Brother to me in person;AbdulrasheedAbdulkareem, TaiyeAmusat, Mukhtar M. Kaura, Lukman Sakaand others. My profound gratitude to my friends and cause mates at undergraduate for their contributions to the success of the Dissertation; Dahir Omar Muazu, Abubakar A. Abdulhakeem and Abdulmatin I. Sanni.

In a special way, my profound gratitude and respect to my parent and the entire Bello's family who are all my Brothers and Sisters for their generous disposition and kindness shown on me, no amount of words can equate the generosity and kindness received from them. Thus, I say in all my life that "may Allah, the Almighty reward my parents and my family all abundantly". I shall not forget to thank you in person of;Hawau, O. Aliyu. Thanks for your support all.

ABSTRACT

Satellite Altimetry is an aspect of the microwave remote sensing and space geodesy, used for the study of global mean sea level, sea surface topography,which can be related to the ellipsoid, geoid, wetland water- level monitoring, geophysical exploration and so on. The over flow of water to the Rivers resulted from the rise in Global Mean Sea Level and the changes in the Global Mean Sea Level is better evaluated and understood from a good estimation of reference surface such as ellipsoid and geoid. This study aims at modelling the Geoid heightover the Nigerian Gulf of Guinea Waters fromsatellite altimetry data for a proper understanding of thesurface heights of the Gulf of Guinea relative to the mean sea level using JASON-2 satellite altimetry data.

The data used for the study isJASON-2_GDR (gridded_3×1deg_cycle_mean.nc)products of combined altimetry datasets for a period of seven (7) yearsfrom July 2008 to 2015. The Mea Sea Surface (MSS), theMean Dynamic Topography (MDT) and the Geoid heightwere estimated on latitude -2 to 6 (degree) and longitude 2 to 10 (degree) of the Gulf of Guinea.The sampling was done using Panoply 4.8.3/Java 8 Runtime Environment Software.ArcGIS 10.2.2 software was employed to perform the geo-statistics Inverse Distance Weight (IDW) interpolation for estimatingthe missing points and the Geoid heightsurface modelling/interpolation.

Linear trend analysiswas carried out to estimate the accuracy of measures using Minitab 18 software where Mean Absolute Percentage Error (MAPE) andthe results reveal that, the MSSH, MDT and the Geoid heightwere 2.59269,

1.13365 and 2.66622 respectively.The Mean Absolute Deviation (MAD) for MSSH, MDT and Geoid height were 0.46276, 0.00442 and 0.46532, while the Mean Square Deviation (MSD) wereestimated as 0.34472, 0.00003 and 0.348860 for the MSSH, MDT and Geoid height respectively. The Geoid heightmodels had poor accuracy value with estimate of about 2.7% Mean Absolute Error over the sampled years compared with the MSSH and MDT models of about 2.6% and 1.1% respectively. Theautocorrelation between MSSH, MDT and Geoid heightwere found to be strong with Durbin-Watson value of d = 0.006, which is below the two critical values 0f $1.5 < d < 2.5$.

In addition, the trend for the models were projectedfrom 2016 up to 2022. The MSSH projected an estimate of the range between 17.90m to 19.10m, the MDT projected a range between 0.394m to 0.417m and the Geoid projected an estimate of 16.52m to 18.25m on a sampled data of every July month of the year only. Knowing the trend of the sea surface heights of Nigeria Gulf of Guinea, further research can be carried out to determine how the Nigeria coastal States and climate change can be affected with this trend.

TABLE OF CONTENTS

Page

LIST OF FIGURES

Page

LIST OF TABLES

Page

ABBREVIATION

ADT	Absolute Dynamic Topography
AVISO	Archiving, Validation and Interpretation of Satellite Oceanog-raphic data
CNES	Centre National d'EtudesSpatiales
DT	Delayed Time
DUACS	Data Unification and Altimeter Combination System
DORIS	Doppler Orbitography and Radio-positioning Integrated by Satellite
GDR	Geophysical Data Record(s)
GFO	Geosat Follow On
HY-2A	Haiyang-2A
IGDR	Interim Geophysical Data Record(s)
JPL	Jet Propulsion Laboratory
MAD	Mean Absolute Deviation
MADT	Map of Absolute Dynamic Topography
MAPE	Mean Absolute Percentage Error
MDT	Mean Dynamic Topography
MSD	Mean Square Deviation
MSLA	Map of Sea Level Anomaly
MSS	Mean Sea Surface
NASA	National Aeronautics and Space Administration
NOOA	National Oceanography and Atmospheric Administration
NRT	Near-Real Time

PODAAC	Physical Oceanography Distributed Active Archive Centre
SSALTO	Ssaltomultimission ground segment
SLA	Sea Level Anomaly
SSH	Sea Surface Height
T/P	Topex/Poseidon

CHAPTER ONE

INTRODUCTION

1.1 Background to the Study

The coastal environment has been defined in Cambridge Advanced Learner Dictionary (2008) as “the land next to or close to the sea”. The environment attracts large number of people from different part of the world due to the presence of various kinds of opportunities. These opportunities are products of the activities ranging from tourism, mining, fishery and agricultural operations etc., which are common to coastal environment.

However, “Coast environment” undergoes constant changes every time, due to the dynamic processes that occur around the ocean and sea which is a consequence wave caused by a relative steady winds blowing over the surface of water or unusual meteorological events experienced by the water body. These events include Lanina and El-Niño, whichis caused by changes in temperature of water body, tides due to the gravitational pull of the sun and moon on earth. Pattiaratchi (2011), stated in “Operational oceanography in the 21st century”, that coastal regions experience constant change of rise and fall of sea level at time scales of hours, days, weeks, month annually and etc., governed by the astronomical tides, meteorological conditions, local bathymetry and a host of other factors. The phenomenon known as “mean sea level” (MSL) is usually described as the arithmetic mean of hourly rise and fall of water observed over a specific period of 19

years cycle caused by changing effects of gravitational forces from moon and sun (Fraczek, 2003).

However, the mean sea level is defined as zero surface reference of vertical datum for a local area (Fraczek, 2003). Because of climate change, sea level can rise and could be a serious problem for inhabitants of coastal regions. Sea level rise may cause inundation of low-lying areas, flooding and salt water intrusion into surface water and aquifers (Nicholis, 2010). Furthermore, these effects have a significant impact on national socio-economics, infrastructures and environment due to land-loss around coastal areas where more than 10% of the world's population lives (Handoko*et al.,* 2017).

The Geoid is an equipotential surface of the earth that coincides with the mean sea level. This means that geoid is roughly the sea-level surface when dynamic effects such as waves and tides have been removed or excluded. With the exception of global tide models, which explicitly account for solid earth deformation and changes to the gravity field (loading and self-attraction), most ocean models assume both bathymetry and the z-coordinate to be fixed relative to the rotating earth(Cipollini *et al.*,2013). By definition, geoid describe the irregular true zero surface of the earth for measuring elevations, it is determined by earth gravity and approximated by mean sea level (MSL). Thus, geoid height (N) is the difference between the reference ellipsoid and the geoid, while reference ellipsoid mathematically approximates the surface of the earth.

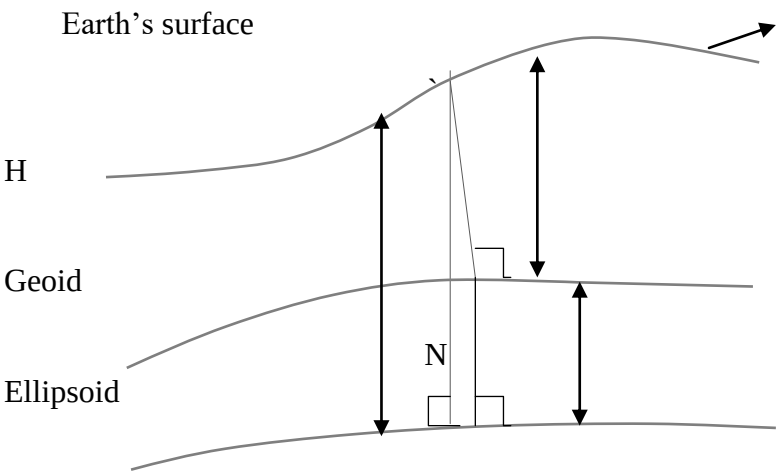

Figure 1. 1. Relationship between References surfaces (Götze and Li, 2001)

Where,

h = Ellipsoid height measured along the ellipsoidal normal

H = Orthometric height measured along the plumb line, and

N = Separation between the Geoid and Ellipsoid (Geoid undulation)

However, the equation that relates these parameters together is given by,(Götze and Li, 2001)

$$h = H + N \qquad (1.1)$$

Space geodesy is a science that employs the technique of remote sensing for measurements or acquisition of information of some attributes of features or phenomena on the earth surface using a recording device that is not in physical contacts with the features or phenomena under study. Multi–mission Satellite Altimetry is one of the products of the space geodesy, which is used to capture information for the study of global mean sea level, sea surface topography that can be related to the geoid, wetland water- level monitoring, geophysical exploration and so on. "With the improvements in

orbit models, radar processing, atmospheric and geophysical effect corrections that have emerged over the years, altimetry gives today a very accurate estimation of the rate of sea level rise and its geographical variability" (Cipollini *et al.,* 2017).

Additionally, some of the multi-mission satellite altimetry were lunched to observe the gravity field of the earth with respect to a reference ellipsoid, and example of these satellites include GRACE (Seeber, 2003). Multi–mission Satellite Altimetry can measure sea-surface topographyrelative to a reference ellipsoid by independently estimatingthe orbit height (H) relative to a reference ellipsoid by precisionorbit determination. The reference ellipsoid measured corresponds to the ellipse thatis closest to the equipotential of the sea surface topography,which is determined primarily by the combined effects of theearth's gravity and centrifugal forces (Dudley *et al.,* 2001). Pail *et al.*(2011), highlighted the recent release of geoid modelsbased on the use of Gravity field andOcean Circulation Explorer data(GOCE),or a combination of Gravity Recovery and Climate Experiment data (GRACE) and GOCE (Bruinsma*et al.,* 2013), which has led to significantimprovements for the calculation of the ocean Mean Dynamic Topography(MDT) at scales (resolution) down to 125 km (Mulet*et al.,* 2012). However, a better accuracy can be obtained as recently carried out by Menna*et al.* (2013), using the approach called "combined geoid models".In the approach, the missing short scales of the geoid are provided by altimeter measurements (by turning theMSS, which is the sum of

the geoid and the MDT, into gravity anomalies that are then used in the calculation of the combined geoid).

According to Rio *et al.* (2014), the accurate knowledge of the ocean's mean dynamic topography(MDT) is a crucial issue for a number of oceanographicapplications based on the use of altimeter sea levelanomalies. The MDT may be calculated as the filtered differencebetween an altimeter mean sea surface MSS – (Schaeffer *et al.,* 2012; Andersen and Knudsen, 2009) anda geoid model.The mean sea surface and the geoid do not coincide because the dynamic sea surfaceheight h_D has both a permanent and a time-variable component. The permanent componentreflects the steric expansion of seawater as well as the ocean circulation that is very nearly in geostrophic balance(Ginzburg*et al.,* 2010).

1.2 Statement of the Research Problem

The economic value of coastal waters and its environment has increased the population of coastal area and also increasedthe coastal activities. As the population continues to grow, more people and property are exposed to severe storms, floods, shoreline erosion and other natural phenomena associated with coastal disturbances which pose potential risk to coastal community across the nation. Powerful storms generate surge waves and currents that can move large amounts of sediment, destroy road, buildings and other critical infrastructures including altering natural habitats. One of the climatic events which produce profound changes on coastlines and

particularly man-made structures in the coastal zone is the hurricanes or typhoons resulting from storm (Scott, 2002).

Moreover, one of the natural phenomena contributing to the disturbances of coastal waters and its environment is the global mean Sea level rise, which is one of the major causes of coastal erosion; it is induced by climate changes, corals and melting of glacia (Mimura, 2013). For example, a study being carried out on global sea level rise has predicted it to accelerate through the 21st century. It was stated that, from 1990 to the last decade ofthe 21st century, a total rise in the range 18 – 59 cm has been projected by theIntergovernmental Panel on Climate Change (IPCC) Fourth Assessment Report(AR4) (Meehl*et al.*,2007). Therefore, if the global sea level continues on this trend, it increases the coastal waters and subjects the environment to the risk of damaging floods and storms.

Nigeria is one of the developing countries vulnerable to climate change impact, especially changes in rainfall because of the exposure to extreme weather event and other atmospheric conditions. Consequently, exposing some towns and cities in Nigeria to recurrent flooding, that occurs mostly during heavy downpours. It has been estimated that a rise in sea level by up to 59cm will see several of Nigerian coastal states being submerged in waters and floods (Onyeka andAdaobi,2008). Such events will no doubt, disrupt the life and occupations of theinhabitants such as fishing, farming etc as well as wreak great havoc on theecological balance (ChidiandOminigbo, 2010). This flooding would wreak havoc to the affected communities and

consequently lead to loss lives and properties. The over flow of water to the rivers resulting from the rise in Global Mean Sea Level and the changes in the Global Mean Sea Level is better evaluated and understood through an in-depth knowledge of reference surface or a well-defined and established datum such as ellipsoid and geoid from which Geoid heightare estimated.

The Federal Emergency Management Agency (FEMA) has stated that the elevations, of land, water, and hydraulic structures (e.g., bridges) are key elements in flood study, and the accuracy to which these elements are determined is a critical factor to the accuracy of the final flood map (National Research Council, 2009). However, these elevations cannot be measured to a high level of accuracy and precision, if the physical reference surface for zero elevation (geoid) and the geometric reference surface of a place is not well defined where the geoidal heights can subsequently be modelled. Hence, this research wouldsolve the problemrelating to coastal flood and erosion bymodellingGeoid heightof Nigeria coastalwaters, which can serve aselevation referencesurface to check and monitor the changes in sea level rise around the region.

In view of the statement of the problem, the study therefore sought to answer the following questions;

i. What is the sea surface heights above the reference ellipsoid and the reference geoid in the Gulf of Guinea?
ii. What is the mean geoidal height of the Gulf of Guinea waters from 2008 to 2016 (July month only)?

iii. What is the relationship between the mean dynamic topography (MDT), mean sea surface (MSS) and the Geoid heightin the Gulf of Guinea?

1.3 Aim and Objectives

1.3.1 Aim

The aim of this study is to model the Geoid heightin the Gulf of GuineausingJASON-2 satellite altimetry data with a view to gaining proper knowledge on the rise or fall of the Gulf of Guinea waters relative to the mean sea level.

1.3.2 Objectives

The objectives are to:

i. Determine the mean sea surface (MSS) and the mean dynamic topography (MDT) on the Nigeria Gulf of Guinea waters.
ii. Model the geoid of the Gulf of Guinea waters from satellite altimetry data for period of 2008to 2015 (July month only).
iii. Model the relationship between MSS, MDT and the geoid over the Nigeria Gulf of Guinea waters.

1.4 Significance of the Study

In recent time, our knowledge and understanding of the dynamic nature of coastal environment has greatly improved resulting from the

development of the awaiting revolutionized multi-mission satellite altimetry techniques to acquire information on the oceans and its environment such as the coast. This technology was use to carry out a nearly global marine gravity field survey across the world oceans to a better accuracy and moderate spatial resolution.Additionally, detailed assessment of sea, ocean and their surroundings can be carried out efficiently with the satellite altimetry techniques. This assessment is difficult and may be impossible with the classical method used in the past for oceanography study or operation, which reveal information about the ocean surface topography (OST), global mean sea level, sea surface heights (SSH), ocean circulation and the salinity contents and other dynamic processes that occur in the coast.

Therefore, knowing the Geoid height ofGulf of Guinea water in Nigeria using multi-mission satellite altimetry technique could make it easy to determine the 3-dimensinal space coordinates of the region's waters and better define the geoid of Nigeria Gulf of Guinea waters. This can be used to improve nautical charts to facilitate efficient ship navigation and improve the transportation of goods on our Gulf of Guinea waters for social and economic development.

Finally, if geoid height can be modelled from known geoid heights, it will improve the application of satellite altimetry in the study of coastal dynamic processes. This phenomenon (coastal dynamic processes) if not checked and monitored, can lead to loss of great number of aquatic life and hectares of land to coastal erosion and flood. Additionally, coastal activities

like fisheries, exploration and construction of coastal structures e.g Inlets, Jetties, Ports and Harbourscan be affected by environmental disturbances. Therefore, to facilitate coastal urbanization development, it is necessary to understand the shape of the coastal waters, rise and fall of the water level and other natural phenomena that affect the coastal waters.

1.5 Scope and De-limitation of the Study

A number of studies have used satellite altimeter data, alone or in combination with other satellite data,forgeophysical study like Sea Surface Heights (SSH). Ocean Surface Topography Mission (OSTM), and Ocean circulation around the Gulf of Guinea region. One of the aspects of geophysical study, which this research is going to look into, is the determination of the Geoid heightfor Nigeria Gulf of Guinea waters using multi – mission satellite data. Although, the SSH measurements from satellite altimetry in Gulf of Guinea region is hindered not only by less reliable geophysical and environmental corrections (Chelton*et al.*, 2001), but also by the noise radar returns from the generally rougher coastal sea states and simultaneous returns from reflective land and inland waters (Featherstone, 2006).

To accomplish this research, geo-potential model such as EGM2008 would be acquired to estimate the equipotential surface of the earth gravity that is closely associated with the location of the mean sea surface. The EGM2008 has been used to calculate point values of geoid undulation on

a1/2° by1/2° degree grid. In addition, the model is complete to spherical harmonic degree and order 2159data, which include Tidal gauges to determine the sea level measurement ofGulf of Guinea waters is considered. This research would not look at the temporal changes, the factors that cause the changes in the mean sea surface heights (SSH) and mean dynamic topography (MDT) of the Nigerian Gulf of Guinea waters.

Ocean tides and solid earth tide have been taken into account in processing the satellite altimetry data (Zwalley*et al.,* 1990). Therefore, the study is limited to describing the theoryof determining the tidal error in altimetry data. This is due to the challenges in accessingcertain tidal information of the area of interestsuch as tidal gauge.

1.6 Study Area

The Federal Republic of Nigeria is a maritime state with a coastline of approximately 853 km. Nigeria lies between latitude 4º and 14º North of the equator and longitude 2º 45' and 14º 30'East of the Greenwich meridian. It is bounded on the west by the Republic of Benin, on the north by the Republic of Niger and on the east by the Federal Republic of Cameroun. On the Northeast border is Lake Chad, which extends into the Republic of Niger and Chad and touches the northernmost part of the Republic of Cameroun. On the south, the Nigeria coastline is bathed by the Atlantic Ocean. Nigeria climate is tropical, characterized by high temperatures and humidity as well

as marked wet and dry seasons. The coastal areas have annual rainfall ranging between 1,500 and 4,00mm(Kuruk, 2004).

Fataiet *al.* (2006) described Nigeria land and it's maritime to occupy a total land and water area of 923,768sqkm, with the area of land being 910,768sqkm while that of water is 13,000sqkm(CIA World Fact Book, 2005). Nigeria exercise sovereignty over its territorial sea which has its breadth up to a limit of 12 nautical miles; Nigeria has its sovereign rights in 200-nautical miles exclusive economic zone (EEZ) with respect to natural resources and certain economic activities, and exercise jurisdiction over marine science research and environmental protection(UNICLOS, 1982). Nigeria's continental shelve extends from the shore to the 200m depth(CIA World Fact Book, 2005).

The Nigerian coastal zone experiences a tropical climate consisting of rainy season (April to November) and dry season (December to March). This climate often causes changes in sea level and consequently changes in major rivers found in Nigeria, which includeRiver Niger and River Benue that form a confluence in Kogi State. The outlets of these rivers and their tributaries are masked by the walls of mangrove. Behind this barrier, calm lagoons extend from the western border of the great Niger. The figure 1.1 below shows the part of Gulf of Guineaof Nigeriathatis consideredin thisstudy, covering geographic coordinates of latitude 2°S - 6°N of the Equator and longitude 2°E - 10°E of the Greenwich Meridian as the effective study area.

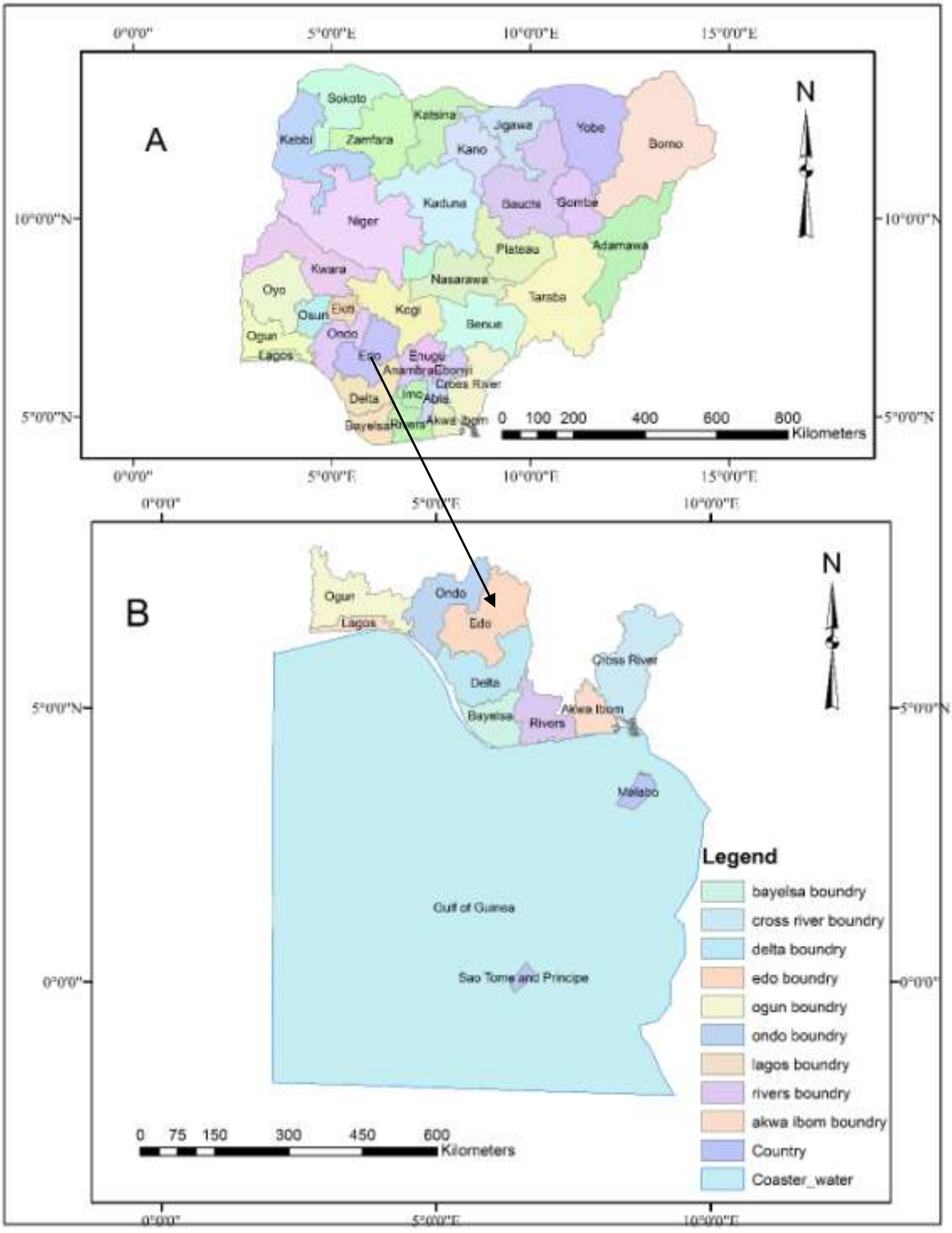

Figure 1. 2. The study Area: (A) Map of Nigeria States, (B) Map of Nigeria Gulf of Guinea (the specified Geographic Coordinates) and theAdjoined Nigeria Coastal State.

CHAPTER TWO

LITERATURE REVIEW

2.1 Theoretical Framework

JASON-2 is a product of satellite radar altimetry and a development in space technology. It provide essential information on solid Earth and Ocean dynamics. Among the information acquired through radar altimetry areMean Sea Surface (MSS) and geoid, which are two key reference surfaces for altimeter data exploitation. Subtractingthe MSS from instantaneous altimeter measurements of the Sea Surface Heights (SSH) yields the Sea Level Anomaly (SLA). Subtracting the geoid from the MSS yields the Mean Dynamic Topography (MDT). MDT and SLA are the twocontributions (the time-mean and the time-variable contributions, respectively) of the absolutedynamic topography from which ocean surface currents can be calculated through the geostrophicapproximation(Escudier*et al.*, 2017).

Satellite Radar altimetry is a technology, which consists of three systems for the determination of satellite's precise location in orbit: the Doppler Orbitography and Radio-positioning Integrated by Satellite package (DORIS, developed by CNES), the Laser Retroreflector Array (LRA, supplied by NASA), and the Global Positioning System Payload (GPSP) receiver (designed by NASA/JPL). The satellite altimeter systemis correctedfrom the instrument errors i.e tracker bias, waveform sampler gain calibration biases, antenna gain pattern, AGC attenuation,

Doppler shift, range acceleration,oscillator drift, pointing angle/sea state. The satellite range (R) which is the measurement from the satellite to the Sea Surface (SS) is determined after being corrected from the atmospheric refraction error (dry gases, water vapor and ionospheric electrons). In addition, the actual measurement for the Sea Surface Height is correctedfrom the Sea-State Bias, which include electromagnetic bias and skewness bias. Finally, the external geophysical adjustment is applied to determine the measurement of the bottom Sea topography as illustrated in Figure 2.1.

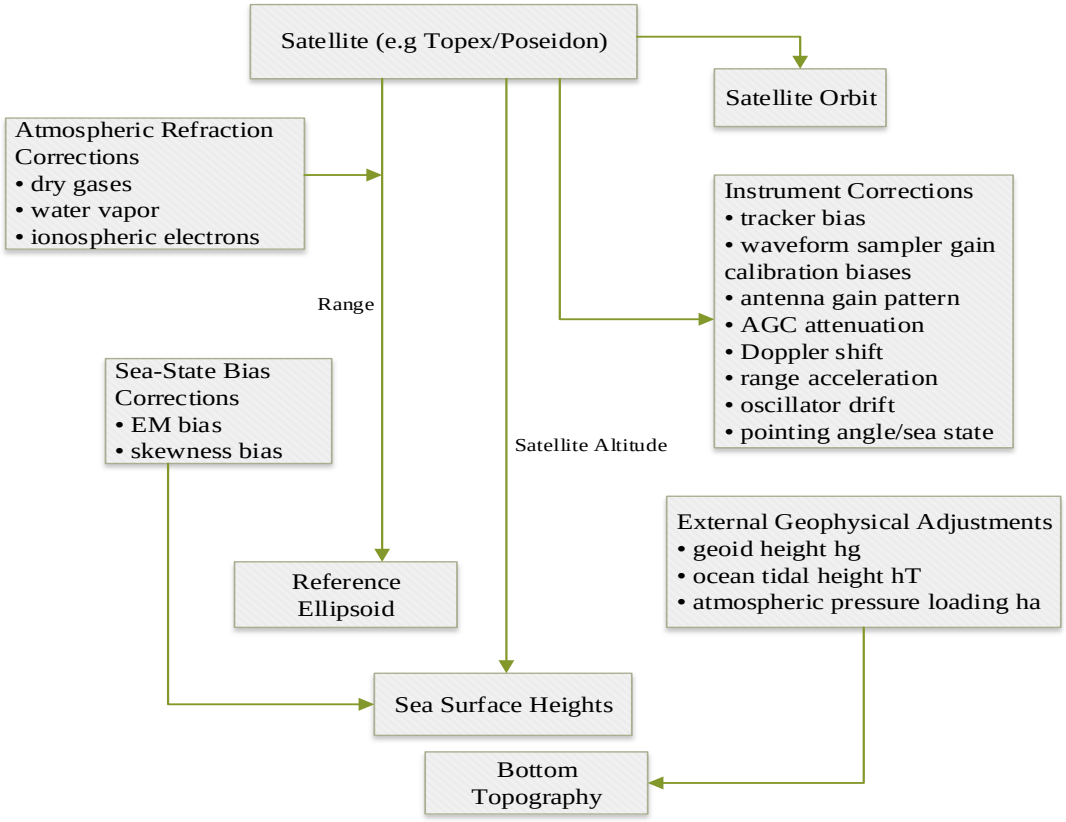

Figure 2. 1.Measurement system of Satellite Altimetry (Source: Cheltone*t al.*, 2001)

2.2 Coasts and Coastal Change

Coastal change poses potential risk to coastal communities across the nation. Powerful storms generate surge waves and currents that can move large amounts of sediment, destroy road, buildings and other critical infrastructures including altering natural habitats. One of the climatic events which produce profound changes on coastlines and particularly man-made structures in the coastal zone is the hurricanes or typhoons resulting from storm (Scott, 2002).

According to Encyclopedia of Coastal Science, the effects caused by the storms are of two types, wind damage and water damage from elevated tides and torrential rains causing coastal flooding. At the center of a hurricane winds it can reach over 200 km/h and storm tides can be as much as 8 m above normal. The amplitude of the storm tide depends on the barometric pressure (the lower the pressure, the higher the tide), the wind speed which causes the water to pile up onshore and the natural state of the tide (i.e., high versus low tide stage). The worst scenario for high storm tides is low pressure and high winds coinciding with a normal high spring tide (Scott, 2005).

2.2.1 Tides

Tides are the periodic motion of the waters of the sea caused by thechanging gravitational effects of the moon and the sun as they change position relative to the rotating earth(Parker, 2007). The gravitational effects or forces arethe same as those causing the moon and earth to remain in their

respectiveorbits.If the Moon and the Sun attracted every water particle in the oceans and seas with thesame force, there would not be any tides. It is the extremely small but perceptibledeviation in the direction and magnitude of the gravitational force of the two celestialbodies upon the particular points on the Earth's surface, which is the cause of the tidalstresses and the tidal phenomena, such as they are observed in nature(Lisitzin, 1974).

The range of tide is defined as the vertical difference in height between consecutive high and low tides, varies from place to place and also over time. By combining the sun-earth system and the moon-earth system, spring and neap tides are developed. Spring tides have nothing to do with springtime. They are tides with ranges greater than the average monthly range. Spring tides occur twice each synodic month due to the approximate alignment of the sun, moon, and earth. Neap tides are tides with ranges less than the average monthly range. They occur twice each synodic month due to the sun, earth, and moon forming right angles (approximately) to each other (Hicks, 2006).

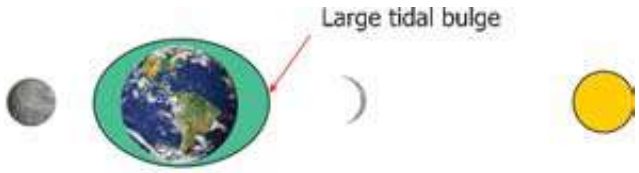

Figure 2. 2. Spring tides - occur at full and new moon(Source: Manley, 2008).

Figure 2. 3. Neap tides - occur at time of half-moon (Source: Manley, 2008).

2.2.2 Ocean tides

In geomatics, measurement of position coordinates, heights, and gravityvalues at points on the Earth's surface, require a corresponding reference surface (datum). A datum could be defined as the base elevation used as a reference from which to reckon heights or depths. Example of datum, which most surveyors are familiar with are Mean Sea Level (MSL), mean lower low water (MLLW) and Mean High Water (MHW). However, datumis defined in terms of the rise and fall or phase of the tide. High Water is the maximum height reached by a rising tide while Low Water is the minimum height reached by a falling tide(Sarah *et al.*, 2015).

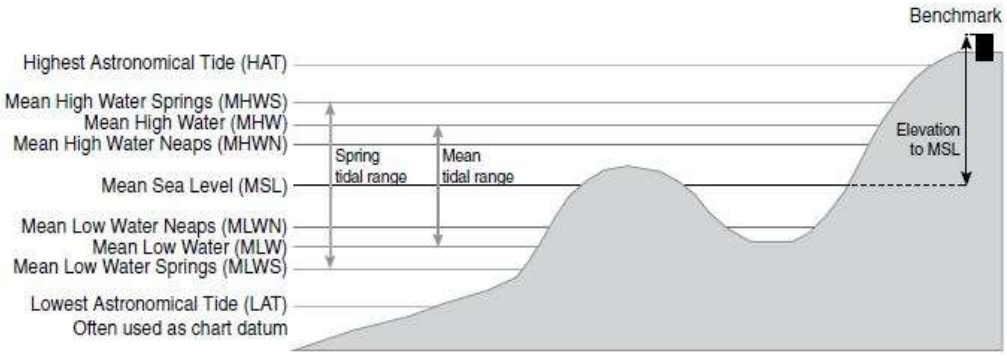

Figure 2. 4. Various tide levels on Ocean (Source: Sarah *et al.*, 2015)

According to Andersen and Scharroo (2011), the altimeter senses the geocentric or elastic ocean tide, which is the sum of the ocean tide andload tide:

$$\Delta h_{\text{elasticocen tide}} = \Delta h_{\text{ocean tide}} + \Delta h_{\text{load tide}} \quad (2.1)$$

This is in contrast to tide gauges fixed to the sea bottom that only measure the oceantide. As the altimeter measures from space, it observes the sum of ocean tide and smallloading displacement of the ocean's bottom due to the loading by the water column. Theload tide has a magnitude of 4−6% of the ocean tide and can be determined by a convolutionof the ocean tide and the response of the upper lithosphere to the ocean loading by that model (i.e ocean tide)(Scherneck, 1990; Agnew, 1997).

2.3. Height System

The height of a point can be describe as a vertical coordinate, which can be measured along a single axis of vertical reference system can be related to gravity when the height axis aligned with the gravity field of the Earth. The classical method of measuring heights such that measurement are taking along the plumb line which everywhere perpendicular to the equipotential surface of the earth gravity field. Usually, height measurements are madeabove a specific reference surface, such asmean sea level(Martin, 2018).

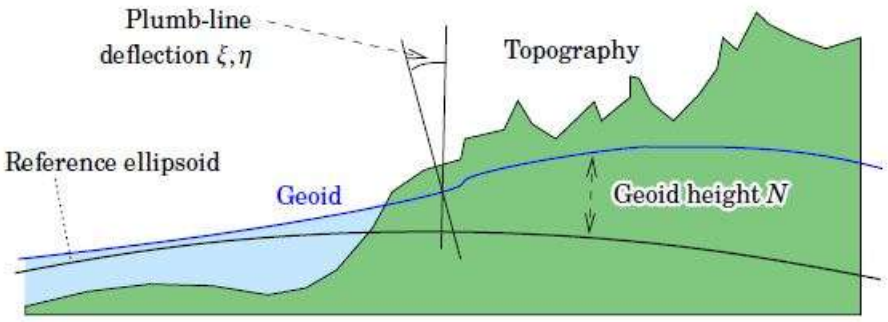

Figure 2. 5.Geoid Heightand Deflection of Plumb line (Martin, 2018)

To obtain difference in height of points, the principle of foresight and back-sight measurement of leveling staff is employed. This technique of height measurement is called leveling. The combination of potential differences which are derived from the height differences measured vertically by spirit leveling with gravity observations are adopted as basic in height systems (Heiskanen and Moritz, 1967). Therefore, height system can be described in its geometric height or physical height.

2.3.1 Geometric Heights

A rotational ellipsoid is a geometric figure obtained by rotating an ellipse around its minor axis. The ellipsoid is having its center and rotation axis respectively coinciding with the origin and the z-axis of the Cartesian system, can acceptablyapproximate the geoid. It is the accurate and computational figure used to represent the figure of the earth in geodeticform.The ellipsoidal height is obtained from GPS observation solution and is purely a geometry quantity. The geodetic height of a point is

the vertical height between the reference ellipsoid and the geoid (equipotential gravitational surface of mean sea level) (Seeber, 2003).

2.3.2 Fundamental relationship of Heights

The distance between the topographical surface of theearth and the mathematical model of the reference ellipsoid surface defined the ellipsoidal height(h). In geodesy, the shape of earth andits external gravity field has been a subject of great importance. Therefore, two assumptions or approximation were made, as a first approximation, the Earth is a rotating sphere. As second approximation, it can be regarded as an equipotentialellipsoid of revolution (Li and Götze, 202).

The ellipsoid revolution is a smooth, regular and convenient surface for mathematical operations. This is why the ellipsoid is widely used as the referencesurface for horizontal coordinatesin geodetic networks (Seeber, 2003).

On the other hand, the ellipsoid is much less suitable as a reference surface for vertical coordinates (heights). Instead, the geoid is used. This is because geoid is defined as that levelsurface of the gravity field, which best fits the mean sea level, and may extend insidethe solid body of Earth(Torge, 2001).

The vertical distance between the geoid and a particular reference ellipsoid iscalledgeoid height or geoid undulation(N). The numerical values of the undulations evidently dependon the particular ellipsoid used and it is

within a range of ±100m. The geometrical relation between the geoid height(N), the ellipsoidal height(h) and the orthometric height, H(obtained from spirit leveling), is shown in the figure (2.1) and the expression below. If any two of the heights are given or known, the third one can be calculated.

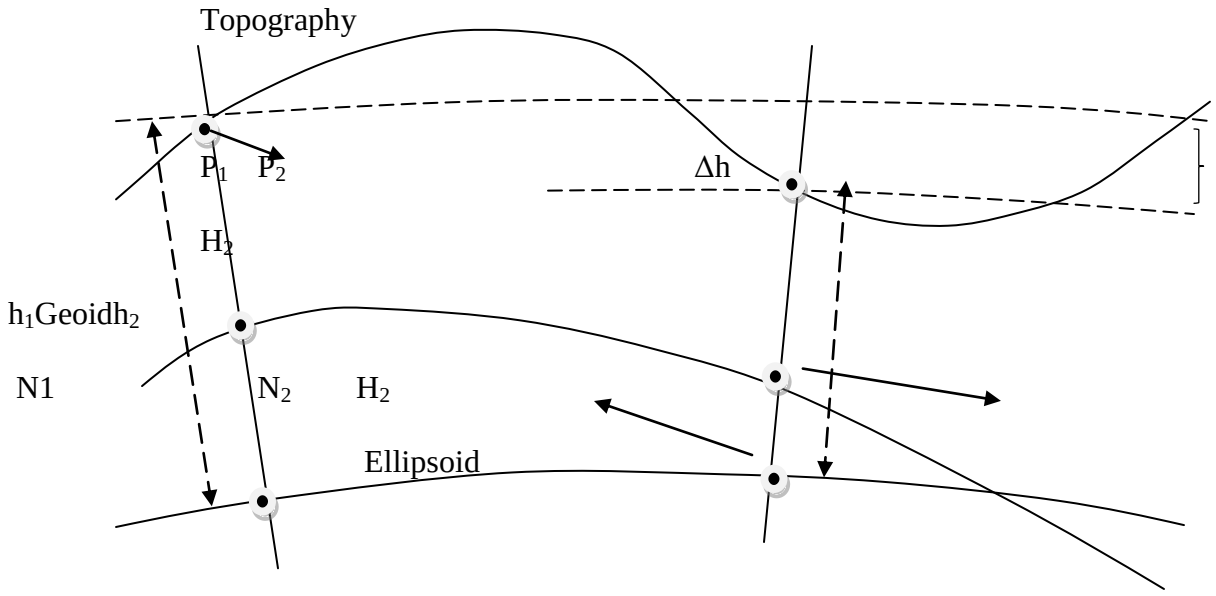

Figure 2. 6.Relationship between heights (Seeber, 2003)

$h1 = N1 + H1;$ $h2 = N2 + H2,$ (2.2)

$\Delta H = H2 - H1;$ $\Delta,h= h2 - h1;$ $\Delta N = N2 - N1,$ (2.3)

$\Delta H = \Delta h - \Delta N,$ $\Delta N = \Delta h - \Delta H,$ $\Delta h= \Delta H - \Delta N,$ (2.4)

Where,

h = Ellipsoid height from GPS observation

H = Othormetric or normal height from spirit leveling, and

N = Geoid height from geoid computation

2.4 External Gravity and Geoid

Gravity can be defined as a combined force exerted on mass due to the gravitation attraction of the earth and the rotation of the earth. The rotation of the earth however has two components: the centrifugal acceleration due to angular velocity (ω) and the existence of equatorial bulge. The study of earth's gravity field is fundamentally a geodetic study to describe the shape of the earth largely by the surface of the ocean, which covers at least ¾ part of the earth (Jekeli, 2007).

One of the significant of gravity is the determination of reference surface for heights measurements, the geoid, as an idealized ocean surface is the level surface if the gravity field. It is important to know that, the terrestrial geodetic measurements are tied on the direction of the plumb line (i.e earth gravity field) with the exception of the spatial distances. This is however, described in a global, spatial Cartesian coordinate system. Therefore, the force lines of the gravitational field (verticals), which are bumpy lines whosedirection changes from point to point, together define the field itself and allow usto describe it through equipotential surfaces, or level surfaces, which areperpendicular to the vertical line at every point (Gomarasca, 2009).

2.4.1 Geoid as reference surface for Heights

A reference system is the set of conventions, measures and rules for the positioning of the terrestrialsurface points in space, according to an established coordinate system (Gomarasca 2009). Once the physical and geometric representations (i.egeoid and ellipsoid respectively) of the terrestrial surface are defined, they can form a reference system and the differencesand the relations among the various reference systems can be established. In points positioning, the geoid–ellipsoid is reflectedrespectively in the solution of the plani-altimetricproblem(Gomarasca, 2009).

The geoid is an equipotential surface approximated by mean sea level surface. Ocean water is considered as freely moving homogeneous matter, which is subject only to the force of gravity field of the earth. Upon attaining a state of equilibrium, the surface of such idealized ocean assumes a level surface of the gravity field (Torge, 1991). The geoid has an irregular shape described as “undulating” due to variations in the Earth’s mass distribution (oceans and land).Consequently, the geoid is not an analytic surface suitable for horizontal reference surface. However, it is well suited as a reference surface for height determination in the gravity field, and easily supplied by spirit leveling in the combination with gravity measurement (Arora, 2011).

2.4.2 Satellite altimetry and geoid determination

The use of satellite radar altimeters to measure global SSH began in l978 with a measurement accuracy of tens of metres and later improved to the

accuracy level of few centimetres in recent years. The satellite or radar altimetry is design to measures the distance between the satellite and the surface below, transmitting radar pulses, the echoes of which are bounced back from the surface, whetherocean, ice cap, sea-ice, desert, lake, or river. This distance, called the range,has two ends. Above the satellite's position is precisely known through orbit determination,referred to the ellipsoid (e.g., WGS84).The on-board navigationdevice such as DORIS or a GPS receiver, or both, make the absolute elevation of thesea surface, land, river, or ice sheet to be derived from the difference between the orbit altitudeand the range, corrected for effects of propagation through the atmosphere and reflection on the surface (Stefano*et al.*,2010).

The observation principle of satellite altimetry is such that, it transmits an electromagnetic pulse to the sea surface and measures its two-way travel time when the return reflected from the instantaneous sea surface is received. The altimeter observed time delay (t) is be converted to the range R from the satellite to the ocean surface as (Lee, 2008):

$$R = \frac{ct}{2} \qquad (2.5)$$

Where, c is the free space speed of the light

The determination of sea surface height from the altimeter range measurement however involves a number of corrections: those expressing the behavior of the radar pulse throughthe atmosphere, and those correcting for sea state and other geophysical signals (Anderson and Scharroo, 2011). The Figure 2.2 illustrates the principle of satellite altimetry.

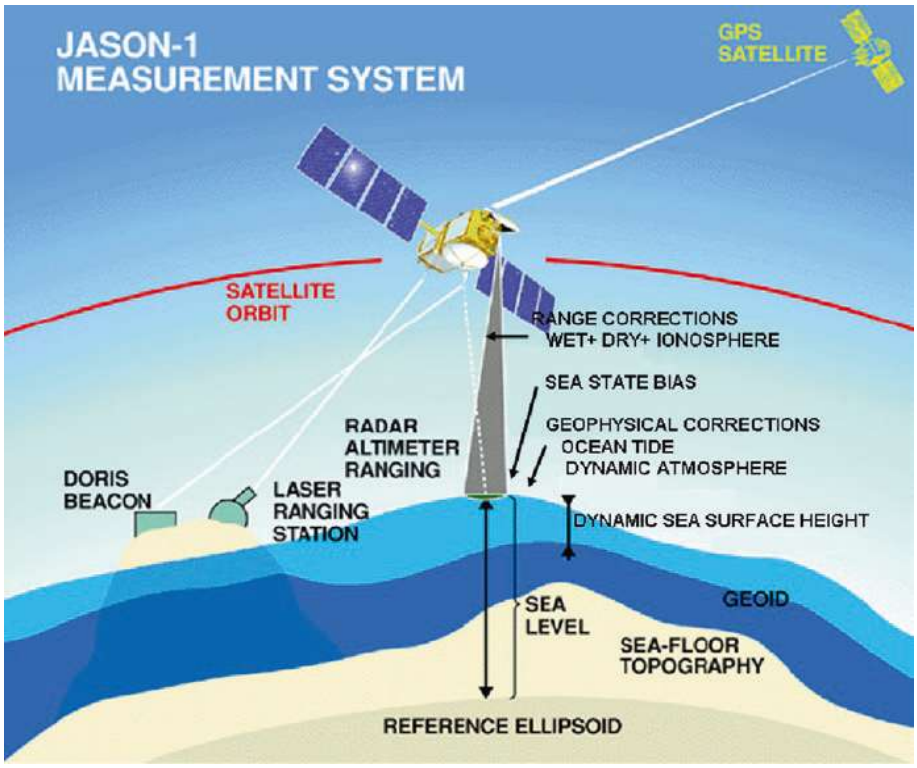

Figure 2. 7:Principle of Satellite Altimetry (Source:Anderson and Scharroo, 2011).

The earth gravitational field is a vector that can be described by a scalar function of space position and time called geo-potential; the value, which are generally obtained through combined leveling and gravimeter measurementtraditionally. However, satellitetechnology has presented a system wheregeoid can be determined from satellite tracking data in combination with surface gravity and ocean altimetry information. The products of this technology is the global geo-potential model derived from Gravity field and Ocean Circulation Explorer (GOCE) and Gravity Recovery and ClimateExperiment (GRACE) missions developed nearly last two decades,examples include EGM96, EGM2008. The accuracy of the geoid is

also fundamental to the precisionof orbit determination and therefore in two ways fundamental to the accuracy of seasurface height observations. With the release of the EGM2008 the RMS uncertainty isaround 10 cm for the ocean (Pavlis*et al.*,2008).

2.4.3 Mean sea surfaceheights

The determination of Mean Sea Surface (MSS) is an important scientific problem in the fields of geoscience andenvironment science nowadays. MSS referenced toan earth ellipsoid contains the information of geoidand Sea Surface Topography (SST), it iswidely used in geoid determination and in the study of sea surface temporal variability, crust movement,ocean circulatione.t.c.Sanso (2002). Also, studies have shown that the mean sea surface mimics the geoid to within a few meters and consequently the two look alike when plotted.According to Peacook and Laxon (2004), the satellite altimeter has been used in the measurement of the time in-variant component of sea surface height or mean sea surface, on a global basis.

According toYahaya*et al.* (2016), the instantaneous height of the sea surface, h_{SSH} at particular time is relative to a reference ellipsoid while the altitude, H_{SALT} of the altimeter above the corresponding reference ellipsoid is given by an independent tracking system (Din and Omar, 2009).

The sea surface height(h_{SSH}), can in its simplest form be described according to the following expression, instantaneous sea surface height(Lee, 2008):

$$h_{SSH} = H_{SALT} - R_{OBS} \quad (2.6)$$

Where,

h_{SSH} = the instantaneous height of sea surface height (SSH) above the reference ellipsoid

H_{SALT}= the altitude of the altimeter above the Corresponding reference ellipsoid

R_{OBS} = the travel time taken from the transmitter to the sea surface and back to the receiver on board.

According to Vignudelli*et al.* (2011), the mean sea surface height is a geometrical description of the averaged sea surface height. However, the mean sea surface and the geoid do not coincide because the dynamic sea surface height $h_{0,}$has both a permanent and a time variable component. The permanent component reflects the steric expansion of sea water as well as the ocean circulation that is very nearly in geostrophic balance. The temporal average of the dynamic topography is called the mean dynamic topography h_{MDT}. The mean dynamic topography is the quantity that bridges the mean sea surface with the geoid height as shown in Figure 2.7, since

$$h_{MSS} = h_{geoid} + h_{MDT} \quad (2.7)$$

Where,

h_{MSS}= Mean Sea Surface height

h_{geoid} = Geoid height

h_{MDT} = Mean Dynamic Topography

ADT = Absolute Dynamic Topography

SSH = Sea Surface Height

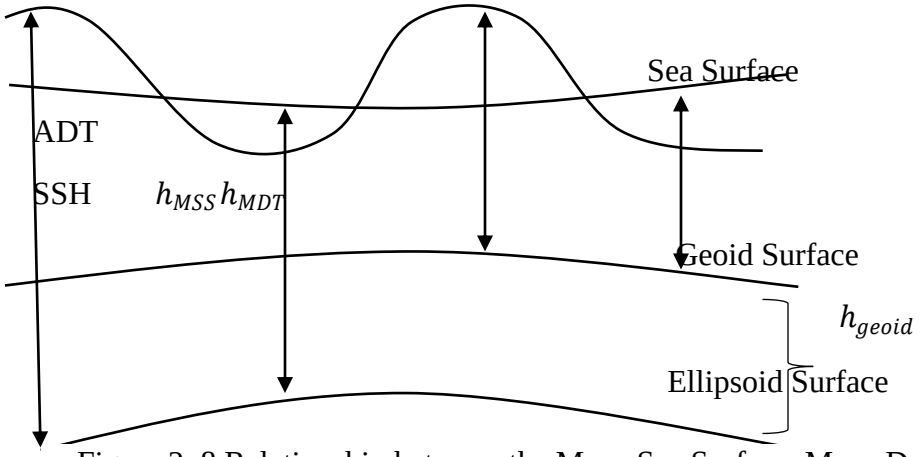

Figure 2. 8.Relationship between the Mean Sea Surface, Mean Dynamic Topography and Geoid height(source: Researchgate, 2018).

2.4.4 Mean dynamic topography

One of the major sources of distortion in verticalcontrol networks is caused by neglecting sea surfacetopography (SST) at tide gauge stations. Often, theorthometric height is fixed to zero at these stationswithout applying proper corrections for thedeviation of the mean sea surface from theequipotential surface represented by the geoid (Fotopoulo*et al.*, 2002).

According to Traon*et al.*(2001), the product that oceanographers will ultimately need from GOCE will thus be a mean dynamic topography (and itserror). Such a computation will require estimating a precise mean geoid for wavelengths larger than 100 to 200 km.This will be best achieved through the

combination of GOCE with GRACE and CHAMP data. This geoid should thenbe subtracted from a very precise altimeter mean sea surface. It will be then necessary to filter the resulting meandynamic topography taking into account the geoid and mean sea surface errors. This mean dynamic topography couldbe in a next step improved using in-situ measurements (e.g. Argo).

2.5 Determination of Tidal Errors and Correction in Altimetry Data

The word ‘tides’ has been defined by National Oceanography and Atmospheric Administration (NOAA), (2000)as the alternating rise and fall in sea level with respect to the land, produced by the gravitational attraction of the moon and the sun. Therefore, tides have been said to contribute greatly to the variability of the sea level measurement. The tidal errors that need to be removed from altimetry data is as a result of ocean tides and earth tides which leads to deviations from an equilibrium surface. Due to the fact that, the effect of tides is dependent on the time of measurement, it is necessary to remove the instantaneous tide components when processing altimeter data, so that all measurements are made to the equilibrium surface (Helen*et al.,* 1999). The estimate of tidal components are made using a combination of numerical tide models and measurement and since, tide varies periodically in a sea level, therefore the differences in tide can be sufficiently determined from long time series of measurement at a given points (Lyard*et al*., 2006). To estimate the ocean tides error and remove them from altimetry data. The

residual ocean tides include the signals with periods of several hours to certain years should be analyzed. Spectral analysis could be used to detect the constituents of the residual ocean tides and the traditional harmonic analysis is used to estimate the amplitude and phase for every constituent that can be distinguished.

Feng, (2012) stated that, before applying any method to analyze the tidal measurements, a very important process is to choose the constituents involved in the estimation. Foreman (1996) suggested there is a maximum of 146 possible tidal constituents that can be included in the tidal analysis; 45 of these are astronomical in origin while the remaining 101 are shallow water constituents. Taking the computation time and the levels of significances of these constituents into account, he created a smaller package of constituents, with an additional 6 long term constituents and 24 shallow water constituents.

However, Ray *et al.* (2011), carried out study on tide predictions in shelf and coastal waters, the study described the Along-track tidal correction on T/P-Jason as an estimates of major constituents where M_2 are now fairly well determined. The mean standard error for T/P-Jason along-track estimates of the M_2 constituent over the global ocean is 0.79 cm, and this number can be somewhat reduced by Along-track smoothing. This error is consistent with, and hence validated by, an analysis of the along-track tide estimates at crossover intersections of independent ascending and descending arcs; the global rms cross-over difference for M_2 is 1.08 cm (roughly $\sqrt{2}$ greater than the mean along-track error, as expected for differences of

independent variates). The largest crossover discrepancies occur in the vicinity of boundary currents, where intense mesoscale variability tends to corrupt tidal estimation. Statistics for constituents O_1, N_2, and S_2 are comparable. Of the major constituents only K_1 appears anomalous, with rms cross-over difference of 2.11 cm, more than twice the M_2rms, presumably a result of cross-correlation between K_1 (alias period 173 days) and the semi-annual cycle of sea level (Ray 1998).

2.5.1 Harmonic tidal constituents

Tides originate from the gravitational forces of the sun and moon acting on a rotating and orbiting earth (Foreman *et al*., 1989). Therefore, tides are caused by both the moon and sun. The contribution to tide by the energy at a particular frequency is usually represented by a tidal harmonic constituent, for which there is an amplitude and a phase lag called an epoch (Parker, 2007). The harmonic analysis approach yields the required amplitudes and phase lags of the harmonic tidal coefficients or any other constituents we may wish to specify. In the case of tidal motions, subtraction of the reconstructed tidal signal from the original record yields a time series generally termed the detided or residual component of the time series. In many cases, it is "detided" signal that is of primary interest (Richard and William, 2014).

Doodson, (1921), showed that all tidal constituents have frequencies that are linear combinations, termed harmonics of the rates of change of r,

mean lunar time, and five astronomical variables that uniquely specify the position of the sun and moon. The astronomic variables are s, the mean longitude of the moon; h, the mean longitude of the sun; p, the mean longitude of the lunar perigee; n', the negative of the longitude of the moon's ascending node; and p' the mean longitude of the solar perigee. The approximate periods for these six variables are 24.84 hours, 27.3 days, 365.24 days, 8.85 years, 18.61 years, and 20932 years respectively. For each constituent, the integer coefficients of these six harmonics are called the Doodson numbers. Therefore, harmonic analysis of tides requires calculating the amplitudes and phases of finite number of sinusoidal functions with known frequencies from a time series of observations (Foreman and Neufeld, 1991). Thus, harmonic tidal prediction involves the summing of a set of cosine curves representing the various tidal harmonic constituents. The table 2.1 shows the tidal constituents and their origin

Table 2. 1. Tidal constituents and their origins (source: Parker et al., 1999)

Symbols	Descriptions	Period	Speed	Derivation From	Coefficient C
Semidiurnal Tides (about twice daily)					
$\mathbf{K_2^L}$	declinational to M_2	11.967 h	30.0821373	$2\omega_L + 2\omega_1 (=2\Omega)$	0.0768
$\mathbf{K_2^S}$	declinational to S_2	11.967 h	30.0821373	$2\omega_S + 2\omega_2 (=2\Omega)$	0.0365
S_2	principal solar	12.000 h	30.0000000	$2\omega_S$	0.4299
M_2	principal lunar	12.421 h	28.9841042	$2\omega_L$	0.9081
N_2	elliptical to M_2	12658 h	28.4397295	$2\omega_L - (\omega_1 - \omega_3)$	0.1739
L_2	elliptical to M_2	12.192 h	29.5284789	$2\omega_{L+} (\omega_1 - \omega_3)$	0.0257
Diurnal Tides					
$\mathbf{K_1^L}$	declinational to O_1	23.934 h	15.0410686	$(\omega_L - \omega_1) + 2\ \omega_1 (=\Omega)$	0.3623
$\mathbf{K_1^S}$	declinational to P_1	23.934 h	15.0410686	$(\omega_S - \omega_2) + 2\ \omega_2 (=\Omega)$	0.1682
P_1	Principal solar	24.066 h	14.9589314	$(\omega_S - \omega_2)$	0.1755
O_1	Principal lunar	25.819 h	13.9430356	$(\omega_L - \omega_1)$	0.3769
Diurnal Tides					
Q_1	elliptical to O_1	26.868 h	13.3986609	$(\omega_L - \omega_1) - (\omega_1 - \omega_3)$	0.0722
Long – period Tides					
Mf	declinational to M_0	13.661 days	1.0980331	$2\omega_1$	0.1564
Mm	elliptical to M_0	27.555 days	0.5443747	$(\omega_1 - \omega_3)$	0.0825
Ssa	declinational to S_0	182.621 days	0.0821373	$2\omega_2$	0.0729

2.6 Review of Related Studies

Frappart*et al*. (2008),carried out satellite altimetry for hydrology. The study determined spatiotemporal variations of water volume over the main stream jointly with the flood plain in the Rio Negro River basin, using area variation estimates for a seasonal cycle captured by the Synthetic Aperture

Radar (SAR) onboard the Japanese Earth Resources Satellite (JERS-1).In addition, the changes in water level from the Topex/Poseidon (T/P) altimetry at eighty-eight (88)altimetric stations, combined with eight (8) in situ liminographic stations was carried out in the study.Water volume variations was determined, the monthly flood period in the Negro River generally ranges from May to August, whereas low-water period ranges from September to February.The results show the high potential for the new technique to provide valuable information to improve our understanding of large river basin hydrologic processes.

Joecila*et al.* (2010), analyze the stages of water bodies in the Amazon basin derived fromfrom the processing of ESRI-2 and ENVISAT satellite altimetry data. Water level time series over river segments of very different width, from the several kilometers to less than a hundred of meters were studied. The result of the comparison at crossovers and with in situ gauges shows that the quality of the series can be highly variable, from 12cm in the best cases and 40cm in most cases to several meters in the worse cases.

Hartanto, (2018), estimated the anomaly of marine gravity field model from satellite altimetry data. Several sets of satellite altimetry data from Cryosat-2, Jason-1 Phase C, Geosat and ESRI were used to compute gravity anomaly over the surrounding waters of Kalimuntan and Sullawasi Island in Indonesia. The altimetry data especially Geosat and ESRI, were retracted to reduce errors due to the land influence. Least Square Collocation (LSC) and Inverse Vening-Meinesz (IVM) method were used for the computation. The

results were compared with the in situ marine gravity data for the National Geophysical Data Centre (NGDC). The results from the LSC and IVM models were compared with root mean square (RMS) error of 10km Gaussian. The Gaussian RMS filtered LSC with RMS error of 15.042mgal, and IVM with an RMS of 16.704mgal.

Ojigi*et al.* (2016),mapped the temporal variability of Absolute Dynamic Topography (ADT) in parts of the Central Atlantic using multi-mission satellite altimetry data for marine and climate change modeling and action plan using LAS 7/Ferret 6.72 interactive software platform. The study showed that,the west coast of Africa (the northern axis of the study area) and the western fringe have relatively higher values compared to the southern and central parts, which were consistently low.The ADT remained consistently high at the coastal region of Nigeria and other West African maritime states with the variation for the period 1993-2016 estimated to be an average increasing rate of about 2.97mm/yr.The study recommend that, time series of the daily/monthly ADT variability in the study area should be evaluated in order to provide the comprehensive trend of the phenomenon for ocean climate change modelling in the region.

Din *et al.* (2014), determine sea level anomaly for Malaysian seas from multi-satellite altimeter missions and investigate the best range and geophysical corrections for Malaysian seas. Sea level data retrieval and reduction were carried out using the Radar Altimeter Database System (RADS). The comparison of near-simultaneous altimeter and tide gauges

observations was carried out at Tioman Island, Langkawi Island and Kota Kinabalu. The results show correlations between monthly values of tide gauge and altimetry data in all selected areas, which are higher than 0.87. These results mean that the altimeter processing did well in this study and the altimetry data has a good potential for sea level anomaly determination using RADS.Multi-mission satellite altimeter provides a means as a complementary tool to the traditional coastal tide gauge instruments in measuring long-term sea level anomaly, especially in a situation where the tide gauge stations are still limited both in number and in geographic distribution.

2.6.1 Inferences from Literatures

The review of the related literatures show the various applications of satellite altimetry technique. These include, satellite altimetry for hydrology, computation of gravity field anomaly, mapping the temporal variability of Absolute Dynamic Topography (ADT), determination of sea level anomaly (SLA) etc. One of the important parameters that can be derived from satellite altimeter is sea level anomaly (SLA), while it is also fundamental for sea level monitoring, geoid determination and current circulations study.

This study therefore, will bridge the gap noted by modeling the geoid heights over Nigeria Gulf of Guinea due to the fact that, geoid heights serve as fundamental reference surface for Geodesists and mapping activities.

CHAPTER THREE

METHODOLOGY

3.1 Research Design and Workflow

The figure 3.2 shows the research workflow, which displayed the sequence of activities performed to achieving the aim of this study. The diagram shows at the start, the JA2_GDR_gridded_3×1_degree_cycle mean (Altimetry Data) that was processed by Panoply to obtain MSSH, MDT and MSSHA datasets and the Geoid extracted. Thereafter, the ArcGIS tool was used to interpolate these datasets. Subsequently, Golden Surfer software was employed to generate contour for surface analysis of the MSSH, MDT and Geoid.

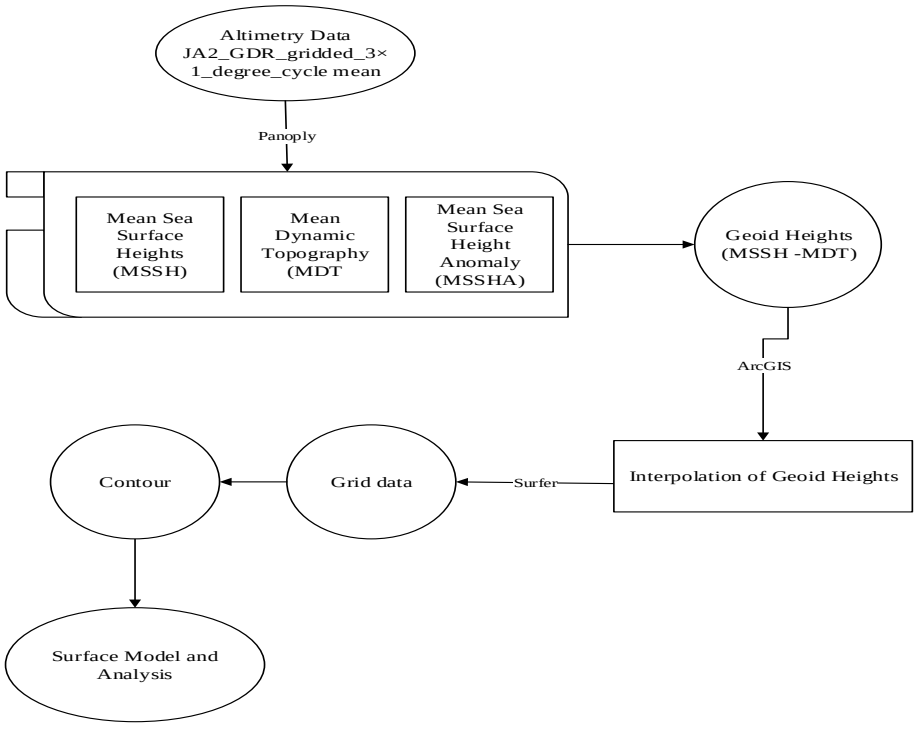

Figure 3. 1. Workflow diagram

3.2 Dataand Sources

The level-2 X-GDR of Jason-2 are available as three data types, which include Operational Geophysical Data Record (OGDR), Interim Geophysical Data Record (IGDR) and final Geophysical Data Record (GDR). The GDR version of Jason-2 was used in this study, and it is based on final high-precision Doppler (DORIS) ephemeris, final meteorological grids, and ancillary and auxiliarydata files.The GDR Jason-2 is available in NetCDF format, and the datasets contained include;

i. Mena Sea Heights
ii. Mean Dynamic Topography
iii. Sea Surface Heights Anomaly and etc.

The GDR JASON-2 data was therefore,accessed from the following websites:

i. http://www.aviso.oceanobs.com.index.php?id=1458/05.26.2017

Instructions for data access are included in the JASON-2 User's handbook and can be found at the following sources

i. ftp://avisoftp.cnes.fr/AVISO/pub/jason-2/documentation/handbook/05.26.2017

As illustrated in Table 3.2, the three families of GDRs, distinguished byincreasing latency and accuracy, going from the Operational GDR (OGDR), to the Interim GDR(IGDR), to the final GDR. Within each of these three families there are up to three types of files inNetCDF format, with increasing size and complexity:

i. A reduced 1 Hz subset of the full dataset in NetCDF format (O/I/GDR-SSHA);

ii. The native NetCDF formatted datasets (O/I/GDRs) which contain 1Hz records as well as 20 Hz high-rate values;

iii. An expert sensor product containing the full radar-echo waveforms in NetCDF format (SIGDR/S-GDR, not applicable to the OGDR) (Source: J2_handbook)

Table 3. 1. OSTM/JASON-2 level-2 products

OSTM/JASON-2	OGDR Family	IGDR Family	GDR Family
Reduced 1Hz	OGDR-SSHA	IGDR-SSHA	GDR-SSHA
1Hz + 20Hz	OGDR OGDR-BUFR	IGDR	GDR
1Hz + 20Hz + waveforms	—	S-GDR	S-GDR
Latency	3 – 5 Hours	1 day	~ 60 days

Size & Complexity

Latency & Accuracy ⟶

(Source: OSTM/Jason-2 Products Handbook, 2011).

3.2.1 NetCDF data format

The netCDF file format and library have been widely adopted by the oceanic and atmospheric communities. It provides a machine independent format for representing array of oriented scientific data. The netCDF provides a very flexible and self-describing data format, for which it includes a header

that gives the layout and other details to the read. The table 3.3 shows the structure of NetCDF files (based on the classic format.

Table 3. 2. Structure of NetCDF Files(Source: unidata, 2012)

Structure	Contents
NetCDF files	Are containers for dimensions, variables and global attributes
Variables	Hold a multi-dimensional array of values of the same type like shape, attributes, values and type
Dimensions	Used to specify variable shapes, common grids and coordinate systems
attributes	Hold metadata (data about data) and contains information about properties of a variables or datasets.
Way to view	CDL (network Common Data form Language) is a human-readable notation for netCDF objects and data

Since netCDF library defines a machine-independent format for representing scientific data, together, the interface, library and format support the creation, access, and sharing of scientific data.

3.2.2 JASON-2 geophysical data record (GDR)

The table 3.3 summarizes the models and standards that are adopted in version “t” product of the OSTM/Jason-2 (O), (I), GDRs.

Table 3. 3. Models and Standard of JASON-2 data

Model	Product Version "t"
orbit	Based on Doris onboard navigator solution for OGDRS. DORIS and laser tracking data for IGDRs DORIS+SLR+GPS tracking data for GDRs.
Altimeter Retracking	"Ocean" retracking MLE4 fit from 2nd order Brown analytical model : MLE4 simultaneously retrieves the 4 parameters that can be inverted from the altimeter waveforms: - Epoch (tracker range offset) ⇒ altimeter range - Composite Sigma ⇒ SWH - Amplitude ⇒ Sigma0 - Square of mispointing angle "Ice" retracking Geometrical analysis of the altimeter waveforms, which retrieves the following parameters: - Epoch (tracker range offset) ⇒ altimeter range - Amplitude ⇒ Sigma0
Altimeter Instrument Corrections	Consistent with MLE4 retracking algorithm
Jason-2 Advanced Microwave Radiometer (AMR) Parameters	Using calibration parameters derived from long term calibration tool developed and operated by NASA/JPL
Dry Troposphere Range Correction	From ECMWF atmospheric pressures and model for S1 and S2 atmospheric tides
Wet Troposphere Range Correction from Model	From ECMWF model
Sea State Bia	Empirical model derived from 3 years of MLE4 Jason-1 altimeter data with version "b" geophysical models
Mean Sea Surface	CLS01
Mean Dynamic Topography	CLS Rio 05
Geoid	EGM96
Bathymetry Model	DTM2000.1
Inverse Barometer Correction	Computed from ECMWF atmospheric pressures after removing S1 and S2 atmospheric tides
Non-tidal High-frequency Dealiasing Correction	Mog2D High Resolution ocean model on (I)GDRs. None for OGDRs. Ocean model forced by ECMWF atmospheric pressures after removing S1 and S2 atmospheric tides

Table 3. 3. Continued

Model	Product Version "t"
Tide Solution 1	GOT00.2 + S1 ocean tide . S1 load tide ignored
Tide Solution 2	FES2004 + S1 and M4 ocean tides. S1 and M4 load tides ignored
Equilibrium long-period ocean tide model	From Cartwright and Taylor tidal potential
Non-equilibrium long-period ocean tide model	Mm, Mf, Mtm, and Msqm from FES2004
Solid Earth Tide Model	From Cartwright and Taylor tidal potential
Pole Tide Model	Equilibrium model
Wind Speed from Model	ECMWF model
Models	Product Version "t"
Altimeter Wind Speed Model	Derived from TOPEX/POSEIDON data
Rain Flag	Derived from comparisons to thresholds of the radiometer-derived integrated liquid water content and of the difference between the measured and the expected Ku-band AGCs
Ice Flag	Derived from comparison of the model wet tropospheric correction to a dual-frequency wet tropospheric correction retrieved from radiometer brightness temperatures, with a default value issued from a climatology table

3.2.3 Accuracy of sea level measurement by Jason-2

The requirement for the Jason-1 IGDR or GDR are derived directly from the post-launch T/P error budget, with the Jason-1 system required to be at least as good as the TOPEX/Poseidon (T/P) system. Each measurement of Sea level shall have an accuracy of ±4.2cm for the GDR products and 5.2cm for the IGDR (1standard deviation) over 1 second averages for typical oceanic conditions of 2msignificant wave height and 11dB sigma-naught. (Bronner*et al.*,2016) This error budget includes the altimeter noise,

uncertainties in orrections of atmospheric path delays, sea state related biases and orbit errors.

3.3 Materials

a. Software

This research used several software tools to produce thefinal results in step-by-step scheme in which different pieces of software had specific tasks and goals.The software employed in this study were obtained from external sources (scientific institutionsor experts). The software employed for the processing of the altimetry data include;Panoply (version 4.8.3), ncBrowse, Microsoft Excel, Broadview Radar Altimetry Toolbox Design (BRAT) Version 4.1.0.

b. Hardware Configuration

The configuration of the computer System (Laptop) used are as follows:

i. System Model: DELL Inspiron N4030
ii. Processor: - Intel(R) Core(TM) i3-2350M CPU @ 2.30GHz,
iii. Random Access Memory (RAM): - 6.00 GB
iv. System Type: - 64-bit Operating System, x64-based processor
v. Hard drive size: - 500 Gigabyte (1 TB)

3.4. Data Preparation, Processing and Computation

The satellite altimetry data used for this research was prepared and archived by AVISO which can be accessed through this address:www.aviso.altimetry.fr. The discussion below state the preparatory steps and computations of some datasets in JASON-2 data used for this study.

3.4.1 Computation of MSSH

The altimeter measures the altitude of the satellite above the earth surface (reference ellipsoid) which are used for the measurement of sea level and consequently sea surface heights. However, the altimeter measurements is perturbed, and affected by geophysical phenomena that include; dry troposphere, wet troposphere, ionosphere, sea state bias, dynamic atmosphere, and e.t.c. and these phenomena need to be corrected from the altimetry datasets. Additionally, the mean sea surface and the geoid do not coincide because the dynamic sea surface height h_D has both a permanent and a time-variable component (Andersen and Scharroo, 2011). However, the equation 3.2 shows the relationship between the mean sea surface, mean dynamic topography and the geoid.

$$h_{MSSH} = h_{geoid} + h_{MDT} \quad (3.2)$$

Therefore, correct value of sea surface heights is computed using the following operation as stated in DT CorSSH and DT SSHA product handbook.

$$SSH = SA - AR - \text{Correction} \quad (3.3)$$

Where,

SSH = Sea Surface Height (the height of the sea above the reference ellipsoid)

SA = Satellite Altitude (the distance of the center of mass of the satellite above a reference point. The reference point will usually be either on the reference ellipsoid.

AR = Altimeter Range (the distance from the center of mass of satellite to the surface of earth, as measured by altimeter

The reference ellipsoid used is the first-order definition of the non-spherical shape of the earth with:

a. equatorial radius of 6378.1363 kilometers
b. flattening coefficient of 1/298.257000000 (Jason-1, Topex/Poseidon, GFO)
c. WGS-84 Equatorial Radius (a) = 6378.1370 kilometers
d. WGS-84 Flattening (f) = 1/298.257223563 (Envisat and ERS).

3.4.2 Computation of MDT products

A Mean Dynamic Topography (MDT) represents the mean sea surface referenced to the geoid and corrected for geophysical effects. MDT is given as a grid with spacing consistent with the altimeter and other data used in the generation of the grid values. The MDT provides the absolute reform surface for the ocean circulation. The Jason_GDR provides a global MDT

model that is a combined recovery several years based on GRACE mission, altimetry and in situ data (hydrological and drifter data).

The Mean Dynamic Topography (MDT) is a key reference surface for the optimal use of altimeter data. It is the missing component that allows us to estimate the ocean absolute dynamic topography (ADT) and the corresponding absolute geostrophic surface currents from the altimeter Sea Level Anomalies (SSHA), (Aviso^{+}, 2014):

$$ADT = MDT + SSHA \quad (3.4)$$

Along-track ADT products are obtained as follows:

$$ADT = SSHA + MDT \quad (3.5)$$

Where, MDT is the Mean Dynamic Topography.

The Mean Dynamic Topography is the part of Mean Sea Surface Height (MSSH) due to permanent currents, so MDT corresponds to the (MSSH) minus Geoid. Since DUACS 2014 version, a new MDT has been used: it takes into account the recent geoid mean field (GOCE DIR-R4) and in-situ dataset, as well as improved processing method. Details are presented in Rio *et al*. (2013).

Note that the ADT products have been computed with consistent SSHA and MDT fields:

$$ADT = SSHA20years + MDT20years \quad (3.6)$$

3.4.3 Computation of sea surface Heights anomaly (SSHA)

Sea Level Anomalies (SSHA) represent the variations of the Sea Surface Heights (SSH) relative to a Mean Sea Surface (MSS). This MSS is representative of a particular period of time, called the reference period. Since 2001, the SSHAs have been referenced to a period of 7-years [i.e, 1993 – 1999]. However, in 2014, with more than 20 years of altimetry measurements available, CMEMS has made Duacs/Ssalto SSHAs on the L3 and L4 level products available with reference period of 20 years [i.e, 1993 – 2012].

Therefore, Mean Sea Surface (MSS) represents the position of the ocean surface averaged over an appropriate time period to remove annual, semi-annual, seasonal and spurious sea surface height signals. Mean Sea Surface is a distance above the reference ellipsoid and is based on seven years of Topex/Posedion data series, five years of ERS data series and two years of GEOSAT data series (reference CLS01, Hernandez *et al.*, 2000).

For most oceanographic purposes, the effects of non-geostrophic processes on the sea surface height will also be removed using geophysical corrections.

Note: all the geophysical parameters here are heights, as defined in figure 3.1, and as such are positive upwards.

Corrected Sea Surface Height = [Altitude – Corrected Range – Solid Earth Tide Height

– Geocentric Ocean Tide Height – Pole Tide Height – Inverted Barometer Height Correction

– HF fluctuations of the Sea Surface].

The figure 3.3 shows the satellite altimetry heights discussed in the section under data processing and computation.

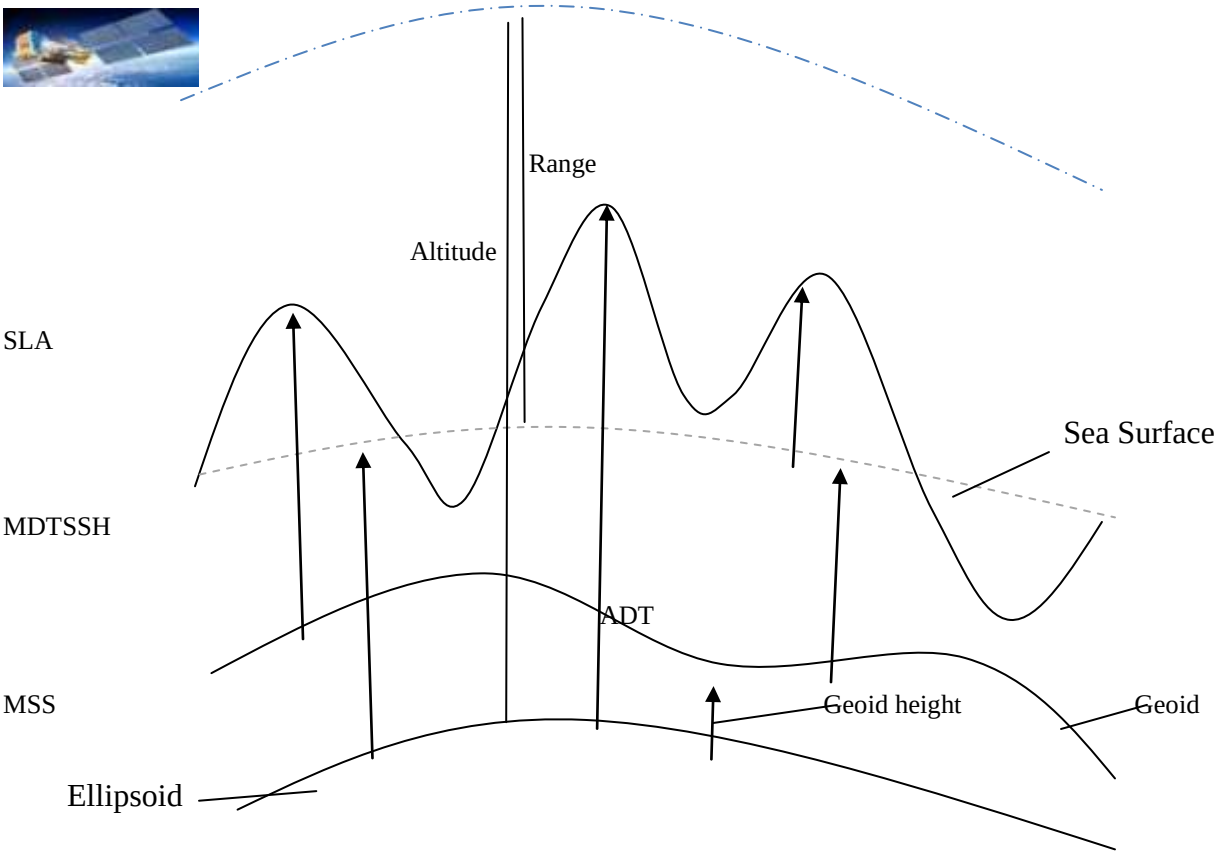

Figure 3. 2. Satellite altimetry heights and their relationship (Source: CNES AVISO^{+})

3.5 Determination of tidal error in altimetry data

The sea surface heights above the reference ellipsoid of JASON-2 altimetry data was determined after applying correction to geophysical errors and consequently, the variable called Sea surface heights anomaly. Tide is the major error in the ocean signal of sea surface heights anomaly. However, the standard approach to determine the tide is called “harmonic analysis” and it is expressed as:

$$\xi p(t) = \sum_n H_n \cos(\varepsilon_n + \sigma_n t - G_n) \quad (3.7)$$

Where

$\xi p(t)$ = value of the variable quantity at time t.

ε_n = epoch determined from luni-solar celestial mechanics.

σ_n = angular speed also determined from luni-solar celestial mechanics.

H_n= local amplitudes to be determined empirically from past records at P.

G_n = phase-lags also to be determined empirically from past records at P.

To determine the error of ocean tides models obtained from satellite altimetry, tide-gauge-derived harmonic constants are necessary to serve as a reference ground truth since they have longer temporal sampling when

compared to the altimetry-derived harmonic constants. Hok (2012), stated that the evaluation of tidal harmonic constant can be made by computing the RMS difference of harmonic constants for each constituent generated (k) from an Ocean tide model against the reference ground truth data, which is defined as (Andersen, 1995b):

$$\text{RMS} = \sqrt{\frac{1}{2N}\sum_{i=1}^{N}\{[C_k^{sol}(i) - C_k^{ref}(i)]^2 + [S_k^{sol}(i) - S_k^{ref}(i)]^2\}} \quad (3.8)$$

Where,

$C_k^{sol}(i)$, $C_k^{ref}(i)$, $S_k^{sol}(i)$ and $S_k^{ref}(i)$ are the in-phase and quadrature amplitude for the ocean tide solution and the reference ground truth data respectively for each location i. N is the total number of locations where the in-phase and quadrature amplitudes are computed. The C_k and S_k in equation above are defined as:

$$C_k = H_k \cos(G_k) \quad (3.9)$$

$$S_k = H_k \sin(G_k) \quad (3.10)$$

Which are called in-phase and quadrature amplitude terms, respectively, that constitutes the tidal (harmonic) constants.

Root Sum of Squares (RSS), accounting for the total deviation of the M major constituents for each model against the reference ground truth data, is an indicator of the overall discrepancy of the model against the reference ground truth, which is defined as:

$$RSS = \sum_{j=1}^{M} \sqrt{RMS_j^2} \quad (3.11)$$

The Root Sum of Squares of the In-phase and Quadrature amplitudes (RSSIQ) for the reference ground truth data over M major constituents is also computed. This served as a denominator for the assessment of the overall fraction of error of the ocean tide models against the ground truth data obtained from RSS, which is defined as:

$$RSSIQ = \sqrt{\frac{1}{2N} \sum_{j=1}^{M} \sum_{i=1}^{N} \{[C_k^{ref}(i)]^2 + [S_k^{ref}(i)]^2} \quad (3.12)$$

As a consequence, discrepancy D is defined as a relative error between the model and the tide-gauge derived harmonic constants, which can be computed as:

$$D = \frac{RSS}{RSSIQ} \times 100\% \quad (3.13)$$

3.6 Geoid Surface Model and Analysis

Surface models allow you to store surface data in a spatial information system. Because a surface contains an infinite number of points, it is impossible to measure and record the z-value at every point. A surface model approximates a surface by taking a sample of the values at different points on the surface and interpolating the values between these points. Geoid height is a 3-dimensional surface (3D), where the heights of the surface correspond to the Z value of the associated grid node and denser grids show greater details on the surface. This study has employed numbers of software

through which Geoid heightis model from satellite altimetry data. The software include

i. Panoply used for taking samples of satellite altimetry datasets like MSSH and MDT from JASON-2_GDR_gridded_3×1_degree_cycle mean data.
ii. Microsoft Excel used for the organizing and analysis of values.
iii. EsriArcGIS 10.2.2 used for the interpolating of sampleddatasets and.
iv. Golden Surfer version 14 used for contour and surface model and analysis.

3.6.1 Sampling of Altimetry Datasets

The grid altimetry data sampling and processing was done interactively using Panoply 4.8.3 software environment (DataOne, 2017).It supports the following operations:

Slice and plot specific latitude-longitude, longitude-vertical, or time-latitude arrays from larger multi-dimensional variables.

i. Combine two arrays in one plot by differencing, summing or averaging.
ii. Plot long-lat data on a global or regional map (using any of over 75 map projections) or make a zonal average data.
iii. Overlay continent outlines and masks on long-lat plots.
iv. Use any ACT, CPT, GGR or PAL colour table for scale colourbar.

v. Save plots to disk GIF, JPEG, PNG or TIFF bitmap images or as AVI or MOV video or as a collection of individual frame images.

vi. Explore remote and open datasets served there.

For the altimetry data to be plotted by Panoply, dataset variables must be tagged with metadata informationusing a convention such as CF.

3.5.1.1 Procedures for sampling Ocean data

The following steps described the procedures used for sampling the Ocean datasets such as MSS, MDT, and SSHA from Jason-1 altimetry satellite data obtained for this study using Panoply software environment, as highlighted below:

Steps:

i. Java 8 Runtime Environment was installed on the computer for the Panoply to work efficiently

ii. Panoply software is launched,JASON-2_GDR_gridded_3×1deg_cycle_mean.nc data is opened with the constituents parameters displayed on the left corner of the software environment.

iii. 2D plot is created where longitude is set for x-axis and latitude for y-axis respectively.

iv. Other settings, whichinclude: Arrays, Scale, Grid, Contours, Vectors and Labels are adjusted.

v. Finally, the values for each datasets like MSSH, MDT and MSSHAcontained in JASON-2_GDR_gridded_3×1deg_cycle_mean.nc is sampled and extracted accordingly.

The table 3.4 shows the grid datasets sampled yearly from 2008 to 2015 of epoch coinciding with July every year. The sampled grid datasets covered an area between geographic longitudes 0 – 12 degree and latitudes -2 to 6 degree of Nigeria Gulf of Guinea waters. Table 3.4 shows the sample datasets from the NetCDF files.

Table 3. 4. Sampled datasets from the NetCDF file.

Jul, 2008					
Long (x)	**Lat (y)**	**MSSH**	**MDT**	**SSHA**	**MSSH - MDT**
0	-2	19.223991	0.34527	-0.041225	18.878721
0	-1	18.83905	0.351698	-0.03785	18.487352
3	0	17.849781	0.37032	-0.05215	17.479461
3	1	17.304174	0.381698	-0.037341	16.922476
6	2	16.473442	0.413175	-0.050667	16.060267
6	3	17.479515	0.407933	-0.039792	17.071582
9	4	19.103485	0.422586	-0.004	18.680899
9	5	—	—	—	—
12	6	—	—	—	—

From the Table 3.5, the longitude 9 to 12 degree and latitude 5 to 6 degree were blank without values. This is because the altimetry satellite could not take any record within the regionbecause; area of land without

Ocean water altimetry data does not capture information of such area.Therefore, has no effect in the computation (i.e blank space in longitude 9 to 12 degree and latitude 5 to 6 degree).

The JASON-2_GDR altimetry data was gridded on three degree intervals along the geographic longitude, which meansdata sample cannot be taken on geographic longitude in between such gridded value (i.e 1, 2, 4, 5, 7, and 8) respectively. It has been discussed in the previous chapter how the geoidal heights is derived and the relationship that connect the MSSH and MDT together.Thus, the column (MSSH – MDT) on the Table 3.4 displayed above represent the geoidal heights.

3.6.2 Inverse Distance Weight Interpolation

To account for the area without samples. This study has considered an Inverse Direct Weight (IDW)interpolation method to estimate and predict missing values and the complete result is given in the appendix.The general equation for the interpolation method is given below

$$z_0 = \frac{\sum_{i=1}^{s} z_i \frac{1}{d_i^k}}{\sum_{i=0}^{s} \frac{1}{d_i^k}} \qquad (3.14)$$

Where,

$z_0$is the estimated value at point 0,

$z_i$is the z value of at known point *i*,

$d_i$is the distance between point I and 0

s is the number of known points used in estimation and

k is the specified power

IDW interpolate a series of point features onto a raster. To process datasets for various points of interest sampled for this study, ArcGIS 10.2.2 software was used to access the spatial and geo-statistic analyst extension for the interpolation. The spatial analyst tools were accessed through the ArcToolbox window and spatial analyst toolbox. The geo-statistical analyst is accessed through the geo-statistical toolbox where the IDW interpolation was performed using the geo-statistical wizard.

3.6.3 Interpolation of JASON-2 Altimetry Datasets

Interpolation of MSSH, MDT heights toestimate the unknown Geoid heightvalues from the limited known dataset of geoid values derived from the summation of sampled MSSH and MDT grid altimetry datasets for the area of interest considered in this study. The study used ArcGIS software for the MSSH, MDT and Geoid heightinterpolation. In the ArcGIS environment, there are tools for various interpolation techniques, which includes Inverse Distance Weighted (IDW), Kriging, Natural neighbor, Spline, Spline with Barriers etc.

The IDW interpolation enforces the condition that the estimated value of a point is influenced more by nearby known points but by those farther away or in other word, to predict a value for any unmeasured location.

3.6.4 The Relationship between MSSH, MDT and Geoid Heights

This study employed regression model methodology to examine the statistical relationship between these three variables (i.e MSSH, MDT and geoid heights), where geoid was made a dependent variable while MSSH and SSHA were made independent variables. This model, show extent to which the geoid (dependent variable) can be predict from the MSSH and SSHA (independent variables). Recall equation (2.5) [i.e., $h_{geoid} = h_{MSSH} - h_{MDT}$], mathematically, the functional regression model for this equation can be written as:

From

$$y = b_0 + b_1x_1 + b_2x_2 + \cdots b_kx_k \quad (3.15)$$

Where,

$y = dependent\ variable$

$x_1, x_2, x_3 \ldots x_k = independent\ variables$

$b_1, b_2, b_3 \ldots b_k = regression\ Coefficients$

Mathematically,

$$h_{geoid} = h_{MSSH} - h_{MDT} \quad (3.16)$$

Then,

$$h_{geoid} = b_0 + b_1(h_{MSSH} - h_{MDT}) + b_2\left(h_{2(MSSH)} - h_{2(MDT)}\right) + \ldots b_k\left(h_{(k)MSSH} - h_{(k)MDT}\right) \quad (3.17)$$

Since, the independent/predictor (MSSH and MDT) variables in equation 3.15 is more than one, then the equation can be referred to as

multiple regression model.The regression model was carried out using IBM SPSS statistics software.Durbin-Watson testwas used to check for the residuals, which is often used to test for positive or negative, first-order, serial correlation. It is based on the assumption that the erros in the regression model are generated by a first order autoreressive process observed at equally spaced time periods.Durbin-Watson testis calculated as follows:

$$\text{DW} = \frac{\sum_{i=2}^{n}(e_i - e_{i-1})^2}{\sum_{i=1}^{n} e_i^2} \qquad (3.16)$$

Where, $e_i = y_i$-$\hat{y}_i$and $y_i$and $\hat{y}_i$, are, respectively, the observed and predicted values of the of the response variable for individual *i*.

Also, the stepwise method of the regression model was selected. This is because at each step, the independent variable not in the equation that has the smallest probability of F-test isentered, if the probability is sufficiently small. Variables already in theregression equation are removed if their probability of F becomes sufficiently large. And the method terminates when no more variables are eligible for inclusion or removal(IBM SPSS User Guide, 2018). In other word, the F-test is to determine whether any of the predictor variables in the model is significant. The significant values in the output are based on fitting a single. Therefore, the significance values are generally invalid when a stepwise method is used.

Finally, the output for the regression model that shows the relationship between the MSSH, MDT and Geoid is presented in chapter

four. This output include descriptive statistics, correlations ANOVA, coefficients andmodel summary and e.t.c.

CHAPTER FOUR

RESULT AND ANALYSIS

4.1 Results

Contour approach was used for the analysis of the result in this study. The contour interval was chosen to allow good interpretation of the models (MSSH, MDT and Geoid) characteristics. Thus, this study chose contour interval of 0.1m for the models of MSSH and Geoid and 0.0025 contour interval chosen for the model of MDT respectively. The choice of the contour interval was due to the fact that, the changes or differences that occurred in the estimated MSSH and Geoid are relatively the same but otherwise as compared to the MDT model.

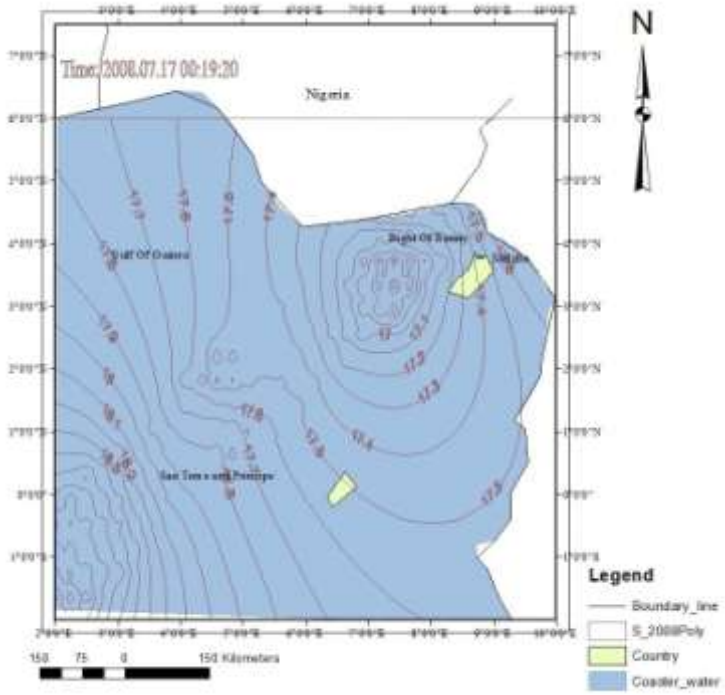

Figure 4. 1a. MSSH July 2008

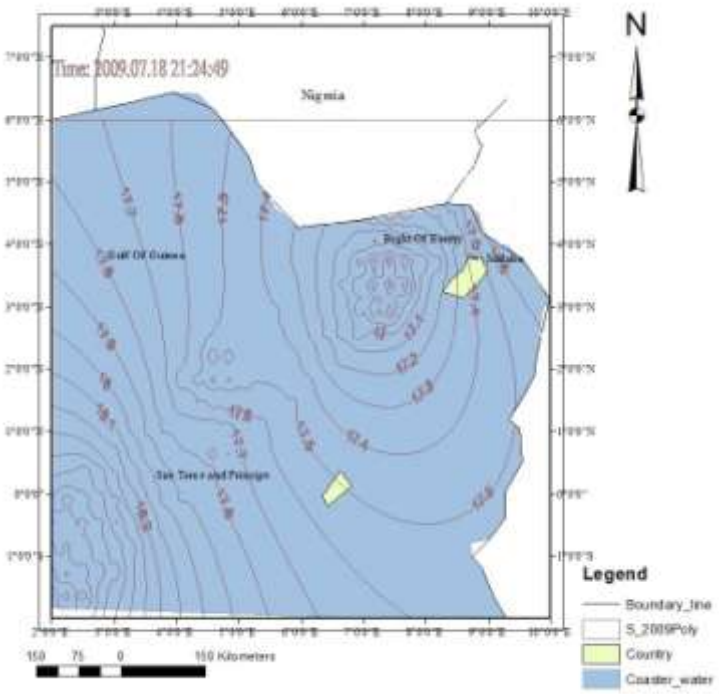

Figure 4. 1b. MSSH July 2009

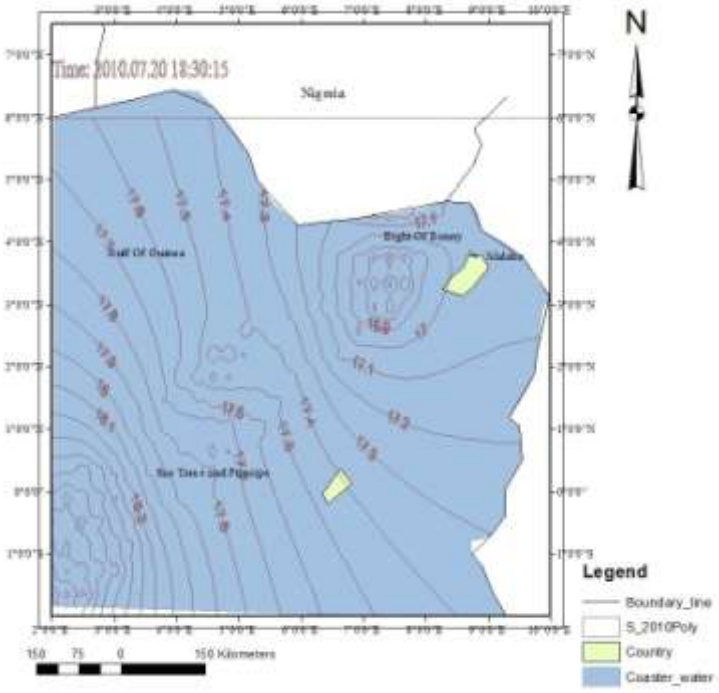

Figure 4. 1c. MSSH July 2010

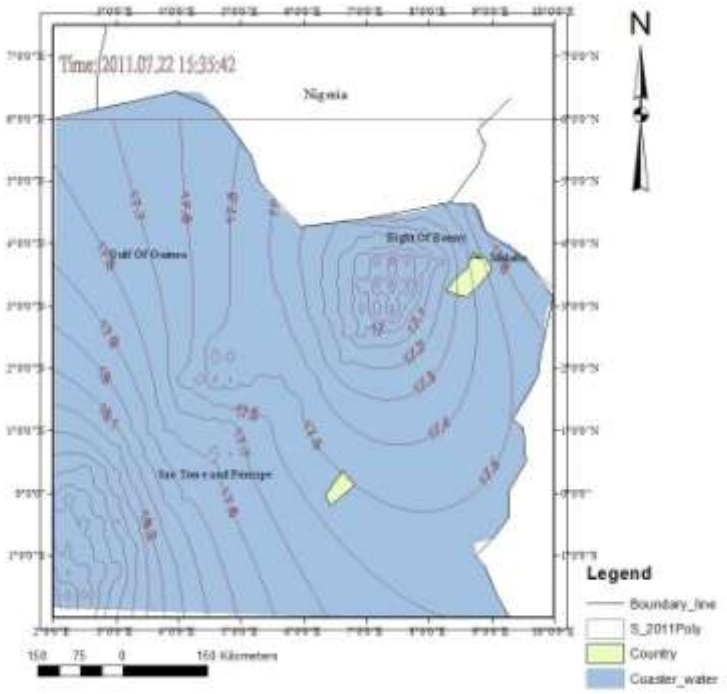

Figure 4. 1d. MSSH July, 2011

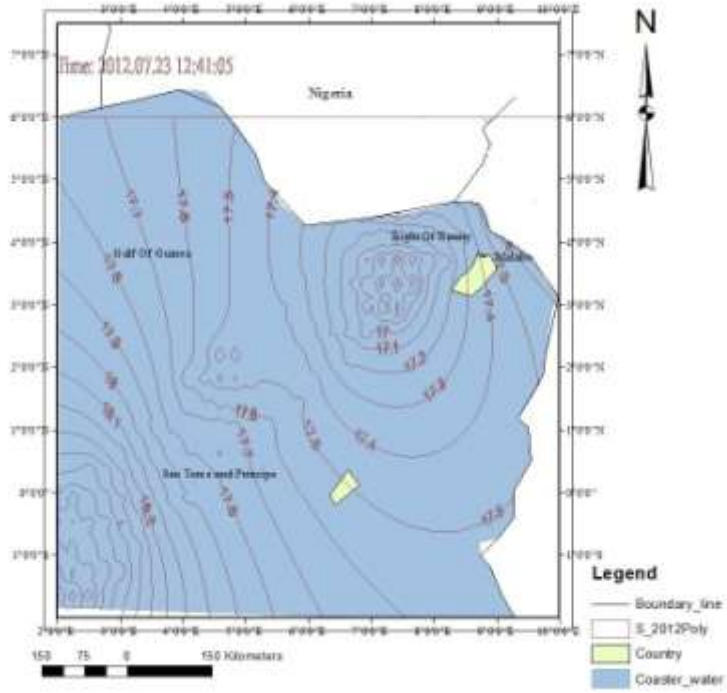

Figure 4. 1e. MSSH July, 2012

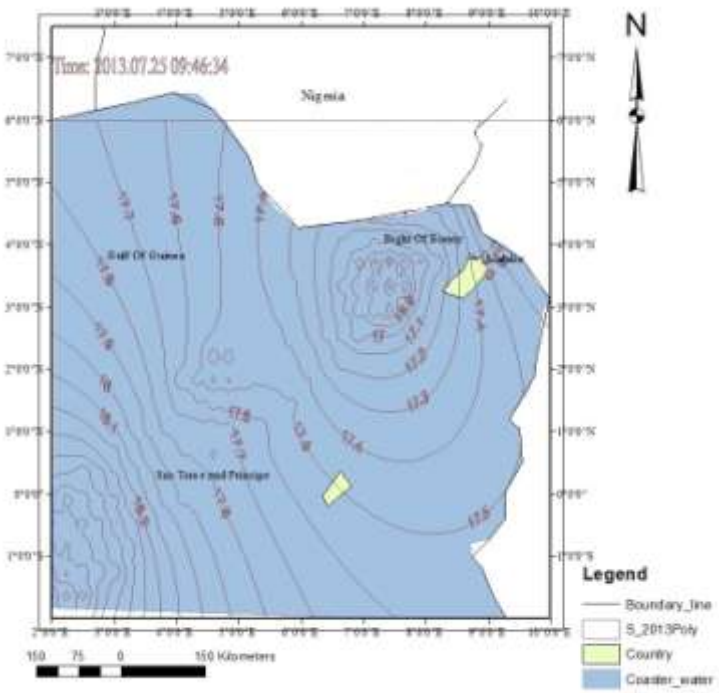

Figure 4. 1f. MSSH July 2013

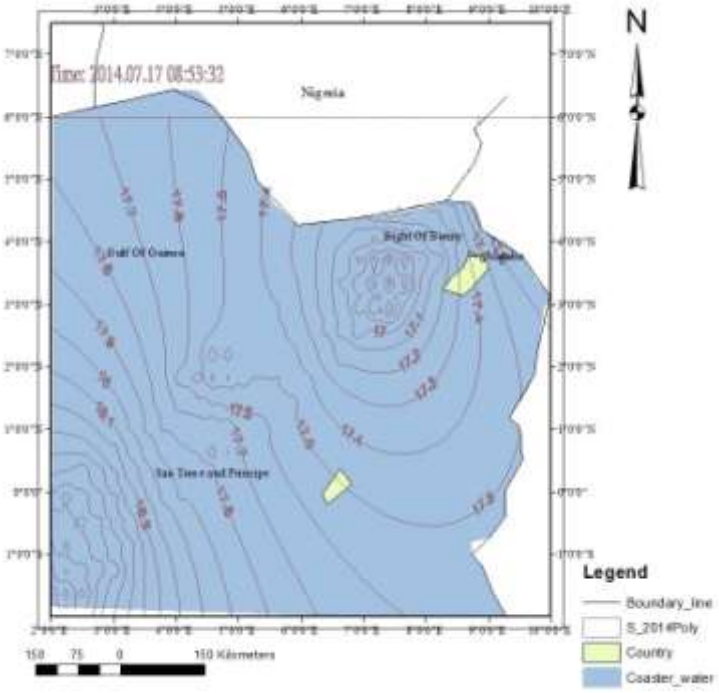

Figure 4. 1g. MSSH July 2014

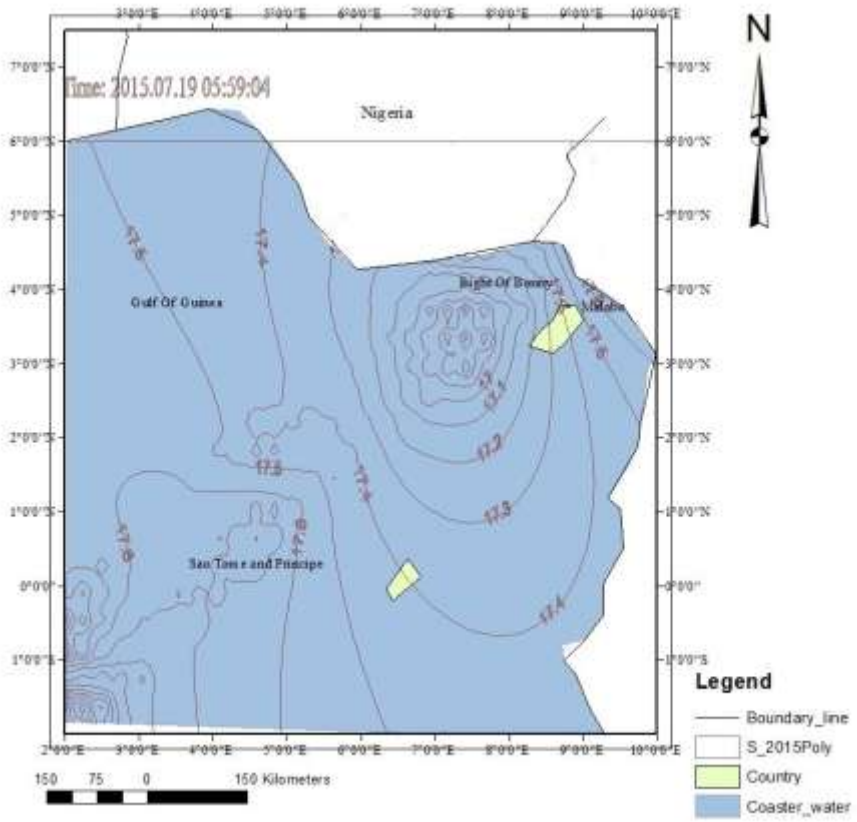

Figure 4. 1h. MSSH July 2015

4.1.1 Analysis of MSSH

In figure 4.1 (a – h), informationabout the MSSH can be deducedfrom the pattern of contour map displayed above. It can be deduced that, regions around 2° north of the equatorto 2.5°south of the equatornear to Sao Tome and Principe recorded a higher level of MSSH with values 18m and 18.2m.Moreover, valuesbetween 17.1mand 17.9m of MSSH isobserved from other part of theGulf of Guinearegion. Additionally, the contour pattern around near the Bight of Bonny show some kind of depression,which translate to MSSH values of below 17m.

Comparing the yearly behavior of the MSSH for the sampled data (i.e an epoch data of only July month yearly) indicates that there is no much significant in the changes of MSSH. However, in 2015, the contour map showed a unique pattern of contour, which indicate significant changes. The contour pattern in 2015 around Lat - Long 6° N - 3° E and 0° N - 6°E including the southern region of Soa Tome Principe shows that there is slightly fall in MSSH as compared to the preceded years sampled.

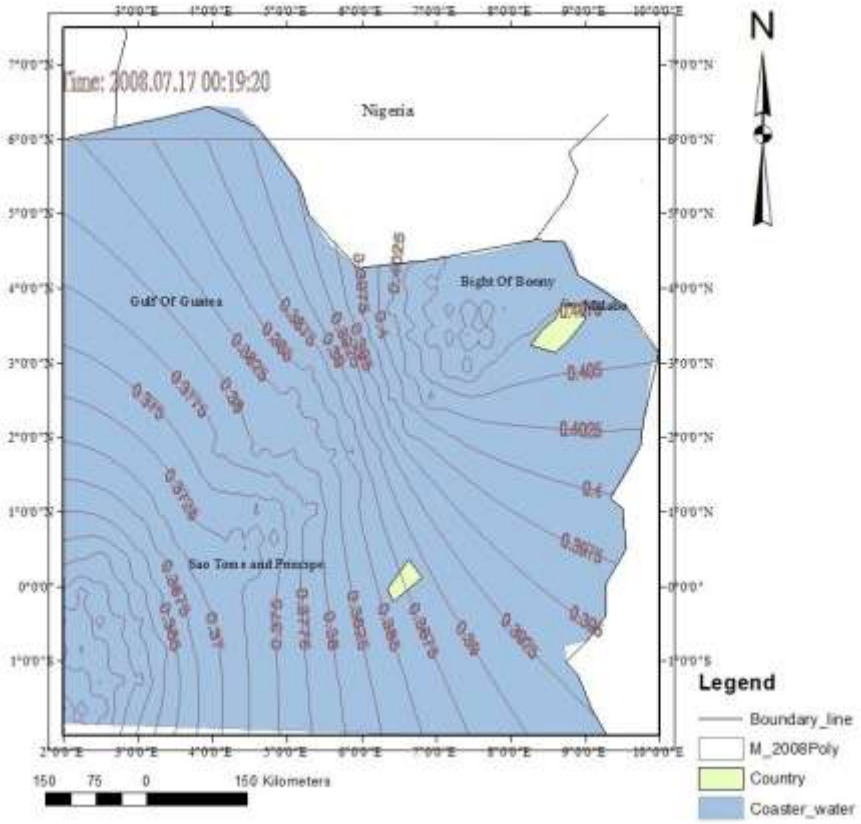

Figure 4. 2a. MDTJuly, 2008

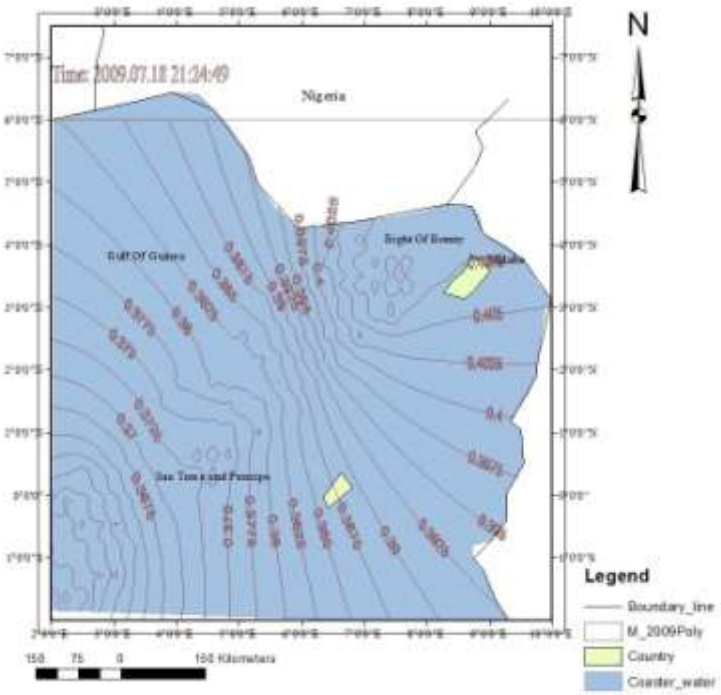

Figure 4. 1. MDTJuly, 2009

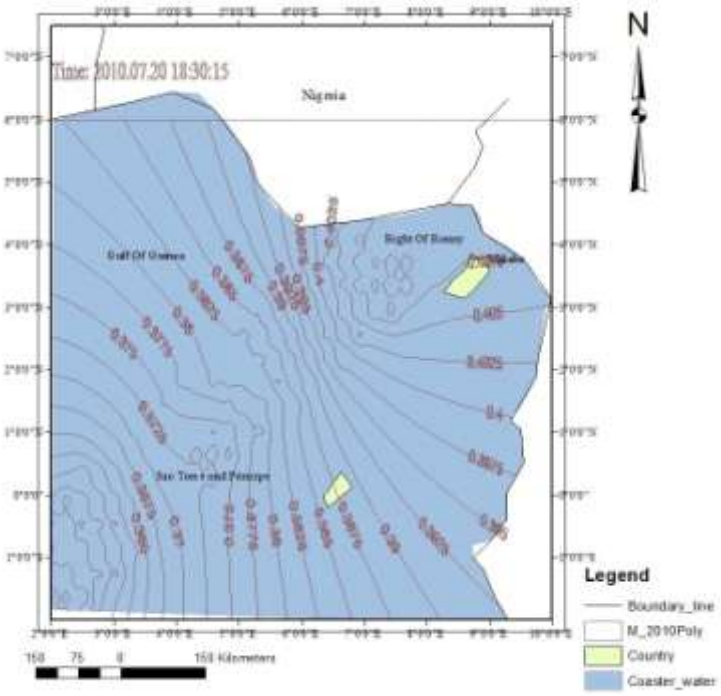

Figure 4. 2. MDTJuly, 2010

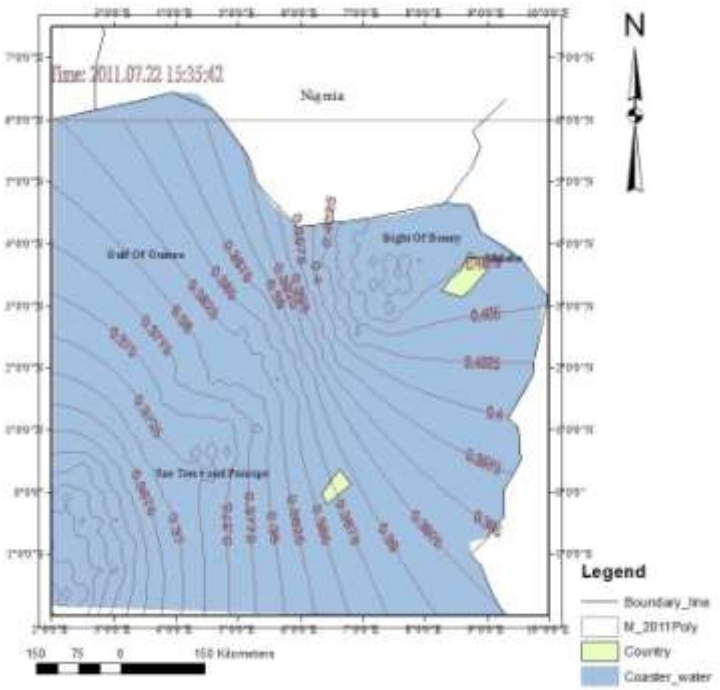

Figure 4. 3. MDTJuly, 2011

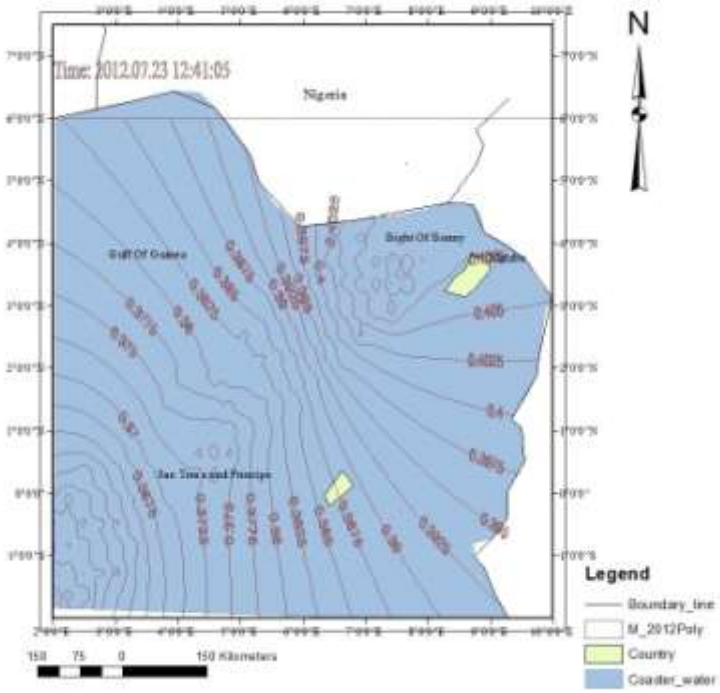

Figure 4. 4. MDTJuly, 2012

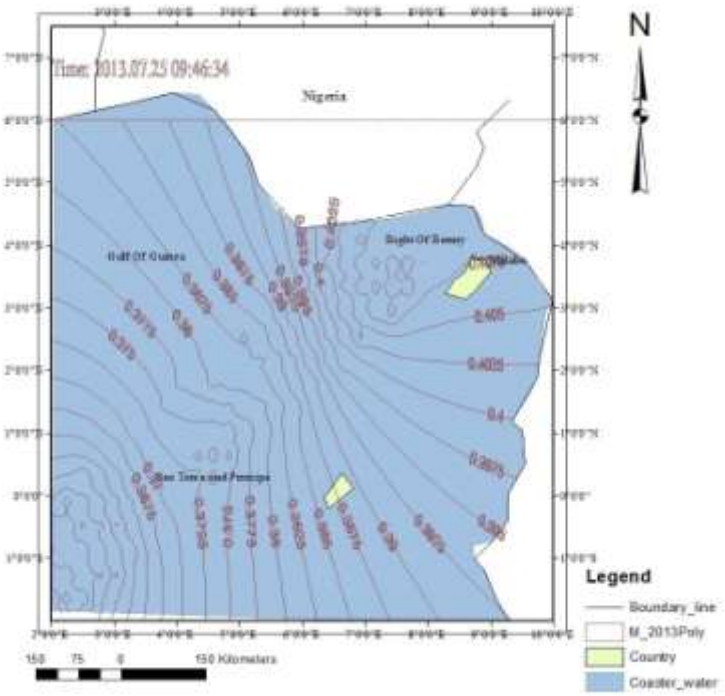

Figure 4. 5. MDTJuly, 2013

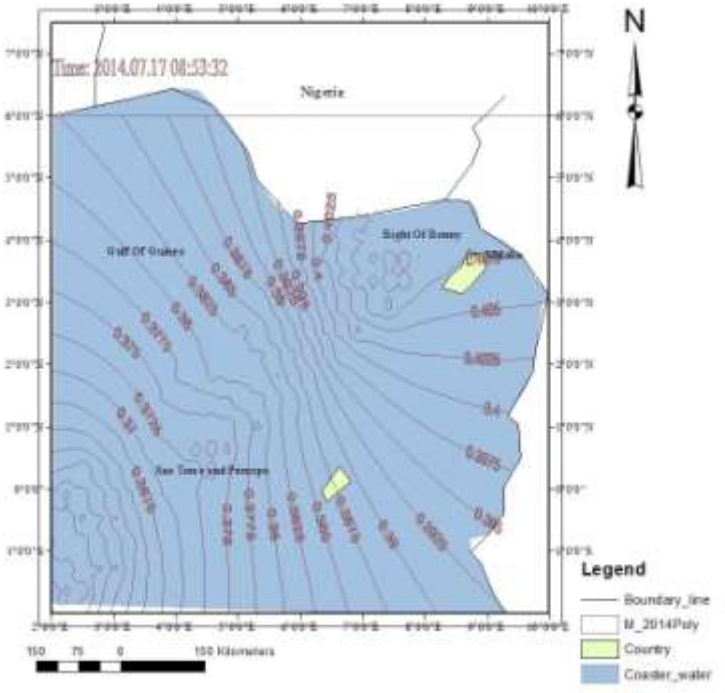

Figure 4. 6. MDTJuly, 2014

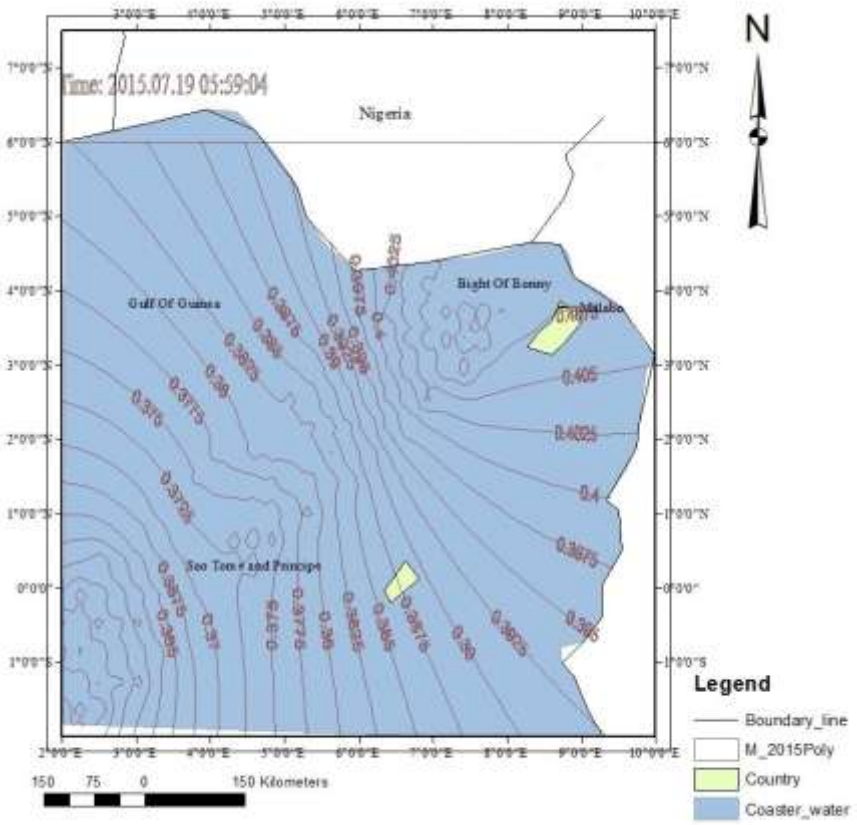

Figure 4. 7. MDTJuly, 2015

4.1.2 Analysis of MDT

The MDT contours through the period of 2008 – 2015 displayed what can be called valley and ridge contour pattern in the form of V or shape.It is observed that, the MDT value of the Gulf of Guinea region nearthe Bight of Bonny and Malaboalong the longitude 6°east of the meridian and latitude 4° down to the latitude 1° north of the equator has the highest values of 0.4m and above. In addition, other regions around the Sao Tome Principe recorded MDT values between 0.37m and 0.39m.This suggest that, the geoid height of these regions (Sao Tome Principe) would be higher than that regions around

Bight of Bonny, Malabo and the specified meridian since, Geoid height is computed from the summation of MSSH and MDT.

Unlike, the MSSH, the MDT does not show any changes in the contour pattern displayed through the sampled year (i.e July 2008 – 2015), and an indication that no much significant changes in the MDT of the Gulf of Guinea Nigeria water.

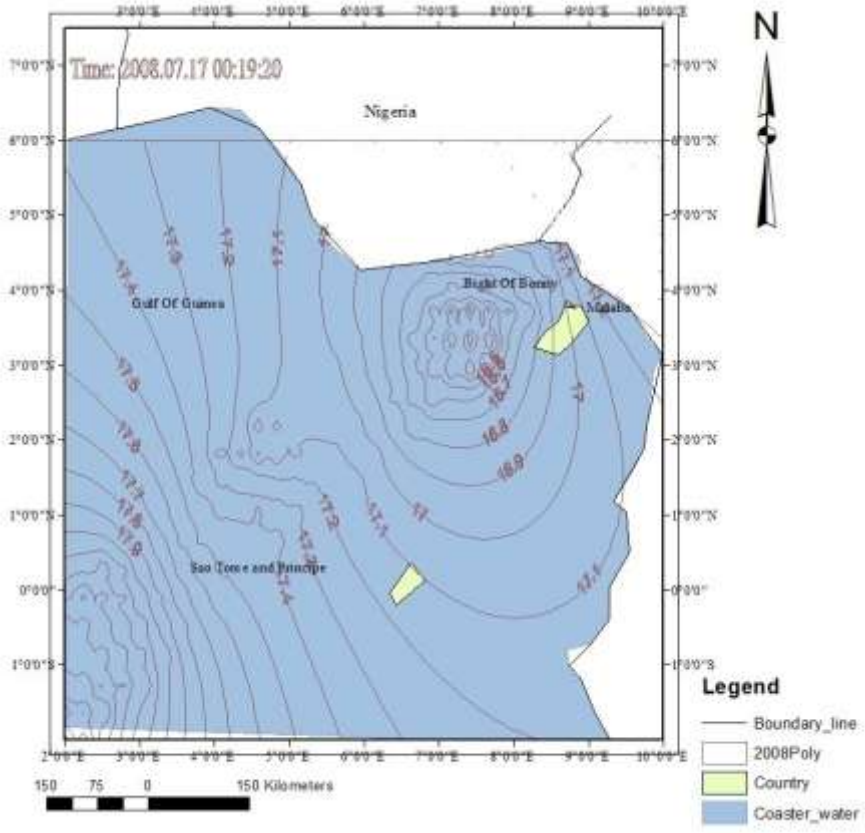

Figure 4. 8.Geoid height July 2008

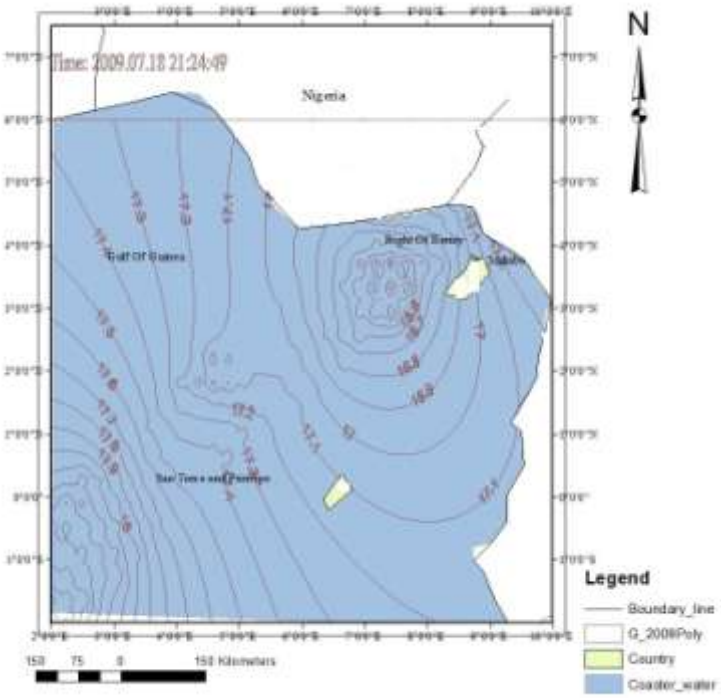

Figure 4. 9.Geoid |HeightJuly 2009

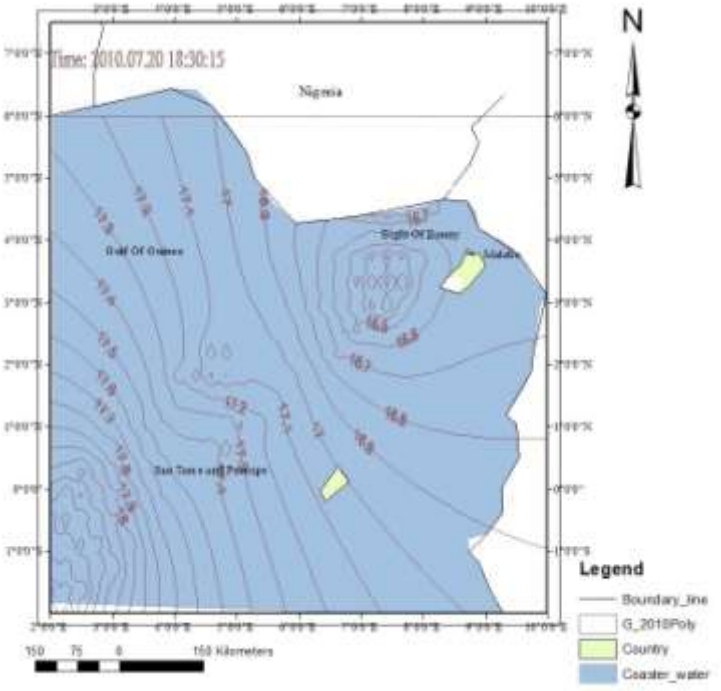

Figure 4. 10.Geoid heightJuly 2010

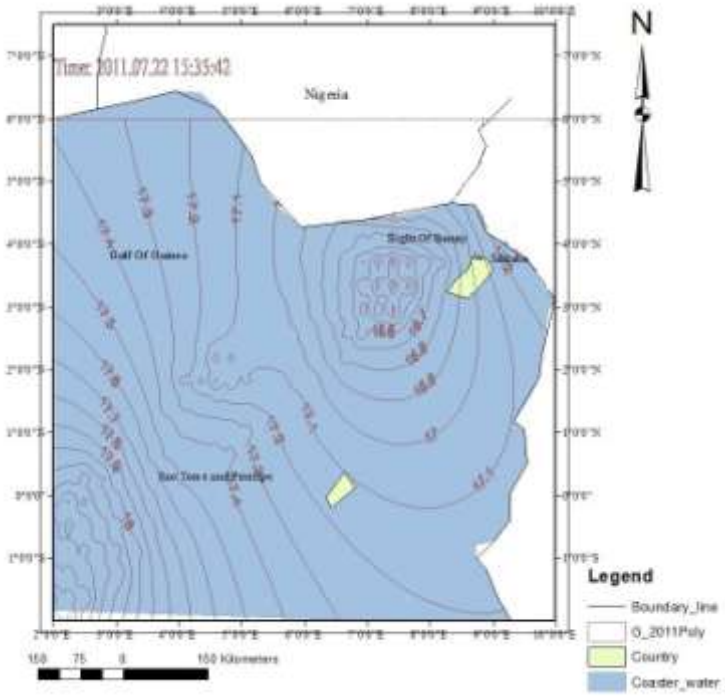

Figure 4. 11.Geoid heightJuly 2011

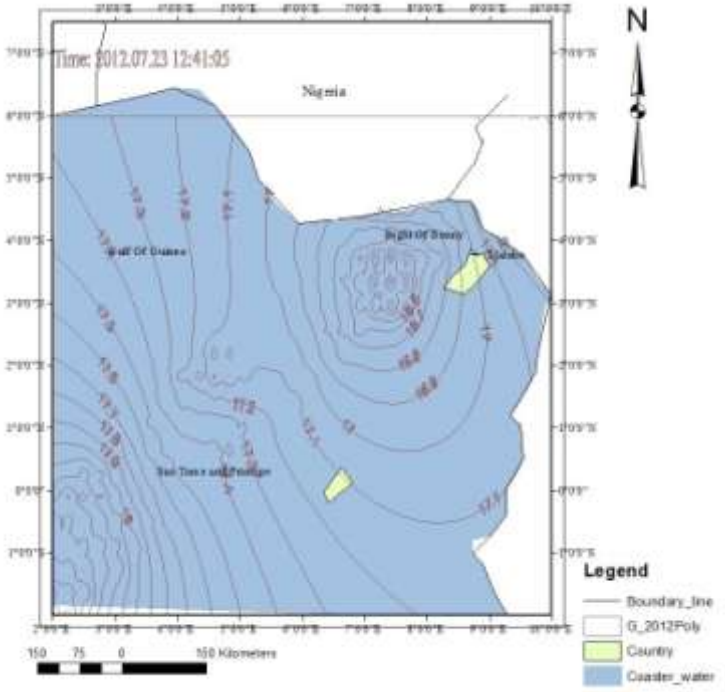

Figure 4. 12.Geoid heightJuly 2012

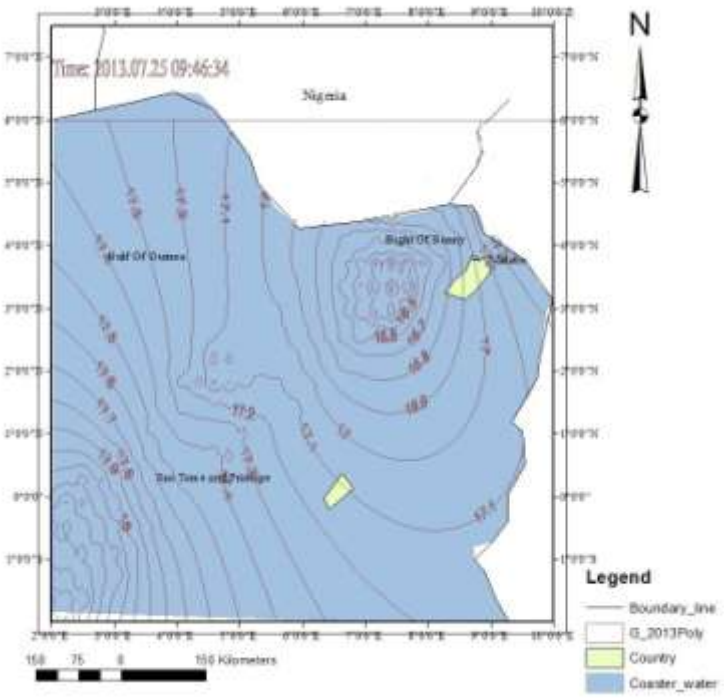

Figure 4. 13.Geoid heightJuly 2013

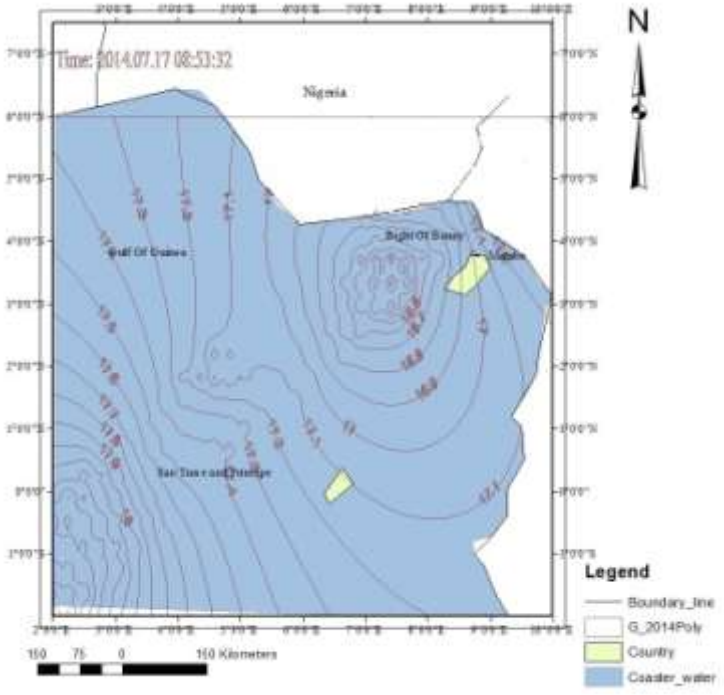

Figure 4. 14.Geoid heightJuly 2014

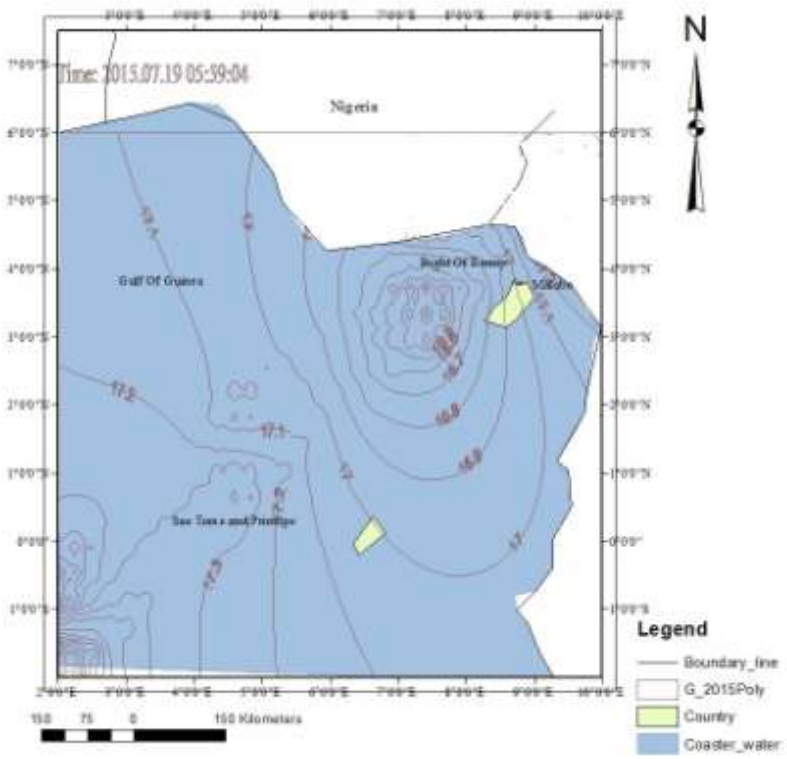

Figure 4. 15.Geoid heightJuly 2015

4.1.3 Analysis of geoid Height

Thecontour pattern of the Geoid model is a representation that shows the contour differences between the MSSH and MDT. Therefore, the value of Geoid around 2° north of the equator to 2.5° south of the equator near Sao Tome and Principe as described and towards the region of Malabo is between 16.7 and 17.4m.

Hence, from the contour maps shown above, obvious differenceswere noticed in the pattern arrangement of contour lines representing MDT from MSSH and Geoid models. For example, the MSH and Geoid models show

some pattern of circles which indicate a depression or a sink, while that of MDT models show some kind of U-shaped pattern that indicate ridges.

In addition, it is important to state that, the two models shown in figure 4.1 (a – h) and 4.3 have adopted a contour intervals of different values to figure 4.2 (a – h). Thesecontour intervals reflect the differences in elevation between two contour lines and changes in gradient values of the two models. Contour interval of 0.0025 was adopted for the MDT model while 0.1 contour interval was used for both MSSH and Geoid model.Furthermore, it is important to note the minimum and the maximum valuesof the scale bar for the models. The MDT scale value is within the range of 0.345 – 0.425, the MSSH is in the range of 16.5 – 19.3m and the Geoid has a range between 16.1 -18.9

4.2 Trend analysis for the MSSH, MDT and geoid Models

Statistical test was carried out and trend analysis was used to model an estimate of gradual changes that occur in the time data seriesof the MSSH, MDT and theGeoid heightmodels from 2008 up to 20015 on Nigerian Gulf of Guinea waters across Latitude -2 to 6 (degree) and Longitude 2 – 10 (degree).The trendof the data series weregeneratedplotted on Minitab 18 software. The graphical plot fortrend of the three models i.e. MSSH, MDT and Geoid respectively is displayed in the figure4.4, 4.5 and 4.6.The graph plots show the linear trend changes, the plots also display the linear trend and

a projection for MSSH, MDT and Geoid over the period of 2016 to 2022 years as sampled from the JASON-2 altimetry data.

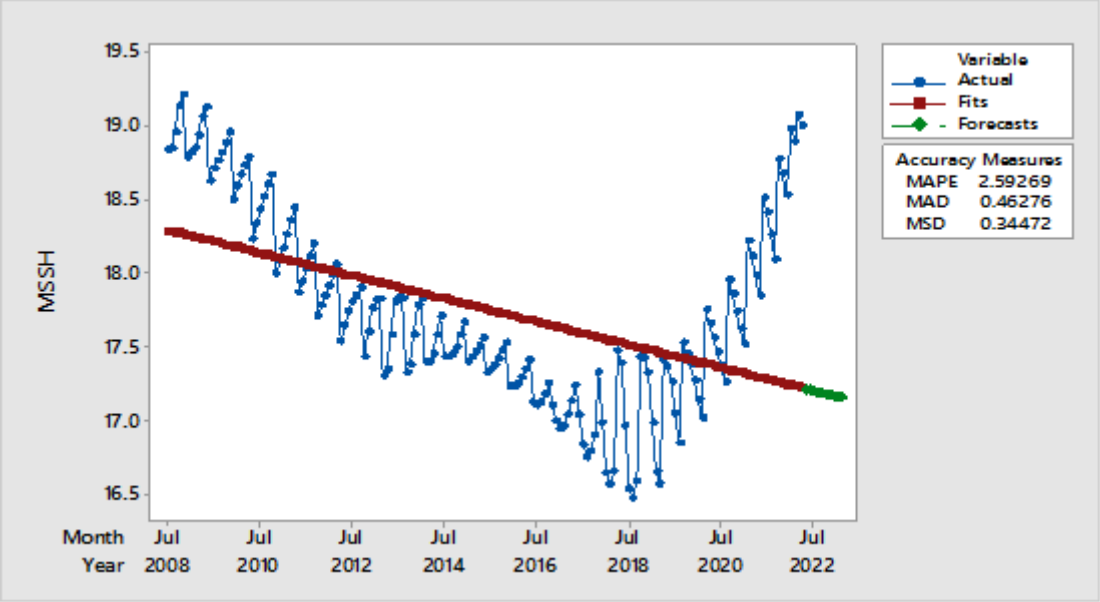

Figure 4. 16. Trend of MSSH in the Gulf of Guinea region of Nigeria (2008 – 2022).

The MSSHgraph plots show a gradual decrease (negative) in linear change is noticed on MSSH. Also, the linear trend model identified the mean absolute percentage error (MAPE) value of MSSH with the lowest value of 2.59, as compared to the MDT and Geoid models with these values 1.13 and 2.67, respectively. From the MPE results, it can be deduced that the MSSH estimated is off by 2.59%, the MDT by 1.13% and the Geoid by 2.67%.

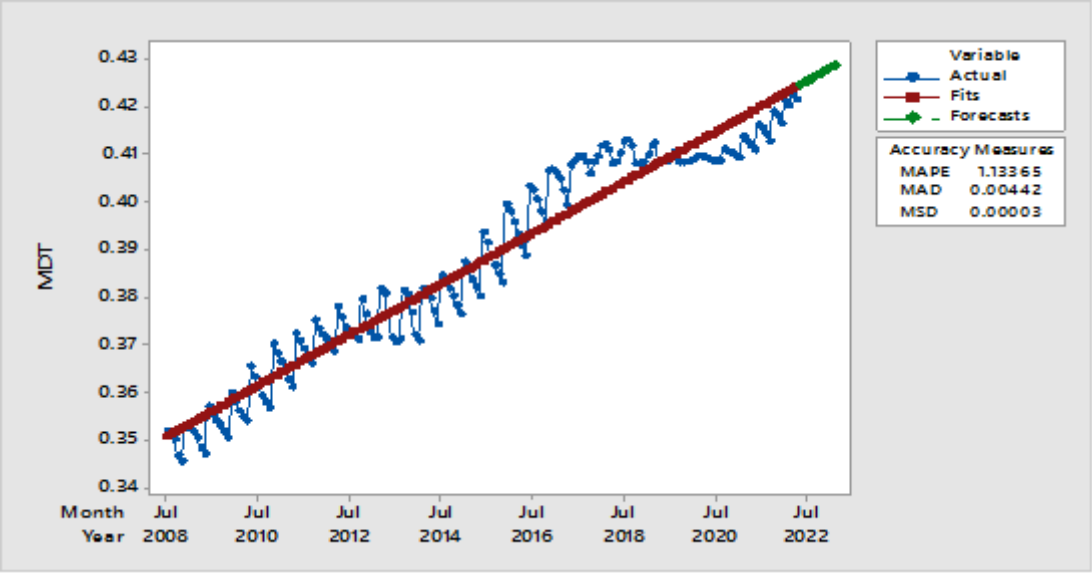

Figure 4. 17. Trend of MDT in the Gulf of Guinea region of Nigeria (2008 – 2022).

The MDT model shows a gradual increase (positive) in linear change. However, the increasing trend rate on MDT is lower comparing to the decreasing trend rate on MSSH. This is evident from the slope of the fit lines on the figure 4.5 and consequently, reflect a relative decrease on the Geoid model.Therefore, it can be said that MDT was estimated with better accuracy for subsequent years as compared to MSSH and Geoid models respectively

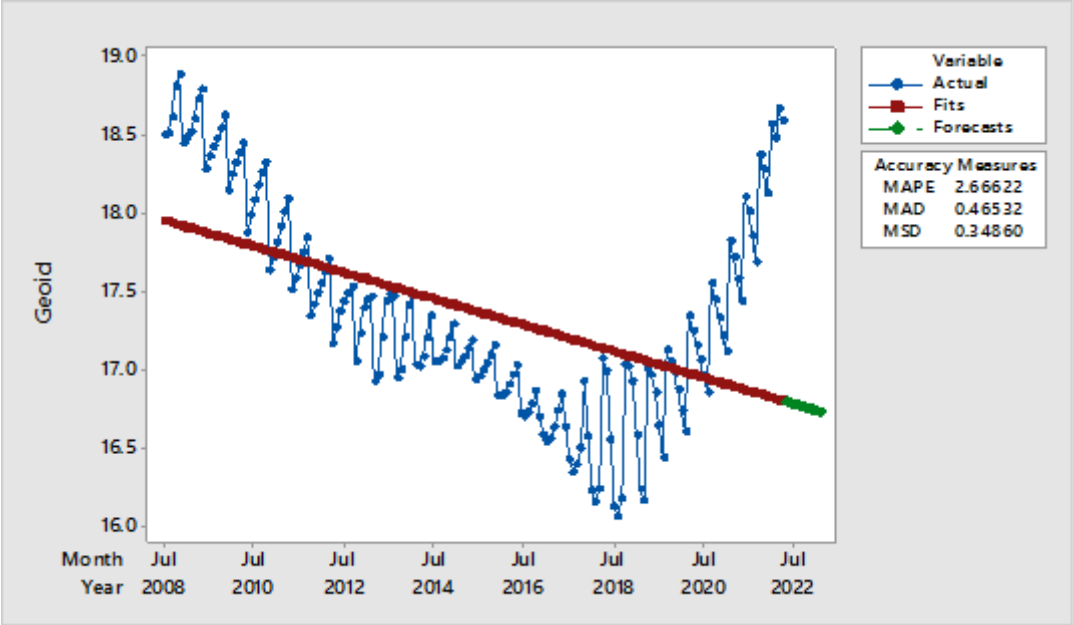

Figure 4. 18. Trend of Geoid heightin the Gulf of Guinea region of Nigeria (2008 – 2022)

Furthermore, comparing the MAD and MSD of the models, the Geoid has a higher values of 0.47,0.35 respectively, while MSSH is low with the values 0.46, 0.34of MAD and MSD respectively. However, the MDTvalues of both MAD and MSDcannot be compared with MSSH and Geoid models. This is because MDT scale is greatly different from both MSSH and Geoid. This scale values can be noticed from the coefficient intercept and the coefficient (t) of the linear trend equations for the models, which is shown in the table 4.1 below.

The time series trend for the models were projected from 2016 up to 2022. The MSSH projected an estimate of the range between 17.90m to 19.10m, the MDT projected a range between 0.394m to 0.417m and the Geoid projected an estimate of 16.52m to 18.25m on a sampled data of every

July month of the year only.Time series equation model (Lineartrend) for the graph plots 4.4, 4.5 and 4.6shows the fitted trend equation,coefficient intercept, coefficient (t) values, fitted equations, and the accuracy measures for each MSSH, MDT and Geoid models respectively of the linear trend model are allgiven in the table 4.1.

Table 4. 1. Accuracy measures of the Linear Trend Model

		Accuracy Measures		
Surface Models	**Fitted Trend Equattion**	**MAPE**	**MAD**	**MSD**
MSSH	yt = 18.3002 – 0.006486 × t	2.59269	0.46276	0.32272
MDT	yt = 0.350369 + 0.000444×t	1.13365	0.00442	0.00003
Geoid	yt = 17.9499 - 0.006930×t	2.66622	0.46532	0.34860

Accuracy measures

i. Mean Absolute Percentage Error (MAPE) measures the accuracy of fitted time series values. It expresses accuracy as a percentage by:Khair, *et al.* (2017).

$$\text{MPE} = \frac{1}{n}\sum\left\{\frac{(yt-\hat{y}t)}{yt}\right\}\ 100 \qquad (4.1)$$

ii. Mean Absolute Deviation (MAD) measures the accuracy of fitted time series values. It expresses accuracy in the same units as the data, which helps conceptualize the amount of error, and is given by: Khair, *et al.* (2017).

$$\text{MAD} = \frac{1}{n}\sum(yt - \hat{y}t) \qquad (4.2)$$

Where in equation (4.1) and (4.2),

yt = the actual value at time t

ŷt = the fitted value, and

n = the number of observations

iii. Mean Squared Deviation (MSD) is always computed using the same denominator, n, regardless of the models(MSSH, MDT and Geoid). MSD is a more sensitive measure of an unusually large forecast error than MAD and is given by: Khair, *et al.*(2017).

$$\text{MSD} = \frac{1}{n}\sum(yt - \hat{y}t)^2 \qquad (4.3)$$

Where,

yt = the actual value at time t,

ŷt= the forecast value and

n = the number of forecasts.

4.3 Relationship between MSSH, MDT and Geoid

The relationship between these three surfaces was discussed in the previous section. However, this study has been able to model (MSSH, MDT and Geoid)the heights on NigeriaGulf of Guinea waters within Latitude -2 to 2 degree north and Longitude 2 to 10 degree east, from JASON-2_GDR_gridded_3×1_degree_cycle mean data on a particular cycle which correspond to July every year were analyzed. The multiple regression model carried out in chapter three above determined the mean and standard deviation of the JASON-2 satellite altimetry data used in this study for the period of 2008 -2015 of a particular epoch in the month of July. A total

number of 1328 data was considered for the model analyses. The table 4.2 in the result output shows the variables thatwere involved in the processesof the analysis of the regression model. It turns out that both MSSH and MDT are useful to predict Geoid.

Table 4. 2. Regression Variables

Variables Entered/Removed[a]			
Model	Variables Entered	Variables Removed	Method
1	MSSH		Stepwise (Criteria: Probability-of-F-to-enter <= .050, Probability-of-F-to-remove >= .100).
2	MDT		Stepwise (Criteria: Probability-of-F-to-enter <= .050, Probability-of-F-to-remove >= .100).

a. Dependent Variable: Geoid Heights

Table 4.3 shows the correlations between the variables, the correlation table can be used to assess the multi-collinearity of the independent variables. For example, if the absolute value of Pearson correlation is greater than ±0.8, then collinearity is likely to exist. However, if the absolute value of Pearson correlation is less than ±0.8, the collinearity is not likely to exist.

Table 4. 3. Regression Correlation

Correlations

		Geoid	MSSH	MDT
Pearson Correlation	Geoid	1.000	1.000	-.621
	MSSH	1.000	1.000	-.600
	MDT	-.621	-.600	1.000
Sig. (1-tailed	Geoid	.	.000	
	MSSH	.000	.	.000
	MDT	.000	.000	.
N	Geoid	1328	1328	1328
	MSSH	1328	1328	1328
	MDT	1328	1328	1328

The Table 4.4 shows the regression model summary and overall fit statistics. The R column of the table shows the values of the multiple correlation coefficient between the predictors, the outcome for both when only MSSH and MSSH & MDT were used is 1.000. It is found that the adjusted R^2 of the model when only MSSH was used in the model 0.999 and it became 1.000 when both MSSH and MDT were involved. This means that the linear regression explains 99.9% and 100% of the variance in the data. The Durbin-Watson d = 0.006, which is below the two critical values of $1.5 < d < 2.5$. Therefore, we can assume that, there is a strong autocorrelation in the multiple linear regression data.

Table 4. 4. Regression Summary

Model Summary[c]					
Model	R	R Square	Adjusted R Square	Std. Error of the Estimate	Durbin-Watson
1	1.000[a]	.999	.999	.017488800483593	
2	1.000[b]	1.000	1.000	.000000028671213	.006

a. Predictors: (Constant), MSSH

b. Predictors: (Constant), MSSH, MDT

c. Dependent Variable: Geoid undulation

The table 4.5 below shows the coefficient of the regression model. From the output, the regression equation can be written as:

Geoid height= 5.984E-14 + (1.000) MSSH –(1.000) MDT (4.1)

And as stated above, the coefficient of multiple determination of the model for both MSSH and MDT is 1.

The variance inflation factor (VIF) measures the impact of collinearity among the variables in the model and it is given as 1/Tolerance. 1.564 VIF for both MSH and MDT were obtained in the regression model carried out for this study, which means that the variables are moderately correlated (that is, there is no multi-collinearity).

Table 4. 5. Regression Coefficients

Coefficients[a]

Model		Unstandardized Coefficients		Standardized Coefficients			95.0% Confidence interval of B		Correlations			Collinearity Statistics	
		B	Std. Error	Beta	t	Sig.	Lower Bound	Upper Bound	Zero-order	Partial	Part	Tolerance	VIF
1	Constant	-.747	.013		-56.771	.000	-.773	-.721					
	MSH	1.020	.001	1.000	1373.130	.000	1.019	1.022	1.000	1.000	1.000	1.000	1.000
2	Constant	5.984 E-14	.000		.000	1.000	.000	.000					
	MSH	1.000	.000	.980	661743560.476	.000	1.000	1.000	1.000	1.000	.784	.640	1.564
	MDT	-1.000	.000	-.033	-22389451.364	.000	-1.000	-1.000	-.621	-1.000	-.027	.640	1.564

a. Dependent Variable: Geoid undulation

Table 4.6: shows the residual statistics based on the regression model. Note, that the unstandardized residuals have a mean of zero, and so do standardized predicted values and standardized residuals.

Table 4. 6. : Regression Residuals Statistics

Residuals Statistics[a]

	Minimum	Maximum	Mean	Std. Deviation	N
Predicted Value	16.07044410705566	18.86842346191406	17.31006131121500	.659460772963510	1328
Residual	.000000000000025	.000000000000039	.000000000000029	.000000000000003	1328
Std. Predicted Value	-1.880	2.363	.000	1.000	1328
Std. Residual	.000	.000	.000	.000	1328

a. Dependent Variable: Geoid undulation

Table 4.7 shows the ANOVA, which reports how well the regression model equation fits the data (i.epredicts the geoid undulation) and is shownin Table 4.7:

Table 4. 7. Regression Anova

ANOVA[a]

Model	Sum of Squares	df	Mean Square	F	Sig.
Regression	577.097	2	288.549	351015853309758590.000	.000[b]
Residual	.000	1325	.000		
Total		1327			

a. Dependent Variable: Geoid undulation

b. Predictors: (Constant), MDT, MSSH

The ANOVA table indicates that both MSSH and MDT in overall regression model predicts the Geoid undulation variable significantly well. This conclusion can be justified, when looking at the "**Sig.**" column over the "**Regression**" row. There is an indication of statistical significance of the regression model that was run, where, $p < .05$

CHAPTER FIVE

SUMMARY, CONCLUSIONS AND RECOMMENDATIONS

5.1 Summary of Findings

The following summarize the findings made by this study:

i. The error in satellite altimetry data is in the range less than ± 0.08m; this was deduced from the value of SSHA displayed in the Appendix A (I to VIII).

ii. The study has shown that the Geoid heightcan be modelled from Satellite Altimetry;hence,geodesists can define the reference ellipsoid and the geoid on Ocean for determination of the shape and size of the earth.

iii. The trend of the sea surface heights were determined, this information could assist us in the monitoring and management of coastal erosion and flooding.

iv. There is a strong correlation between MSSH, MDT and geoid undulation, whereby the MSSH and MDT of a particular region is known then the geoid undulation of that region can be estimated and be modelled.

5.2 Conclusions

The study has modelled the mean sea surface heights (MSSH), mean dynamic topography (MDT) and Geoid heightacross the NigeriaGulf of Guinea waters on latitude -2 to 6 (degree) and longitude 2 to 10 (degree)

from the JASON-2_GDR_gridded_3×1deg_cycle_mean.nc satellite altimetry data over the period of 2008 – 2015.provided by AVISO, Eumetsatand NOOA.

The study has recognized the gradual changes on the MSSH and MDT, which eventually led to the variabilities of Geoid heighton the study area over the period of 2008 – 2015, as Geoid heightwas estimated by subtracting MDT from MSSH. The mean sea surface heights (MSSH) varies between 16.5 and 19.3, and the mean dynamic topography (MDT) varies between 0.345m and 0.425m, hence, the Geoid height varies between 16.1 - 18.9m.The results from the plots show a gradual increase (positive) in linear change,which was noticed on MSSH while the MDT model shows a gradual decrease (negative) in linear change. However, the increasing trend rate on MSSH is higher compared to the decreasing trend rate on MDT and consequently, reflect a gradual increase on the Geoid model. The implications of these changes are that, the Gulf of Guinea regions of the study area may experience consistent high tidal fluctuations caused by rising trend of the mean sea surface height in the study area.

The linear trend model identified the mean absolute percentage error (MAPE) value of MSSH with the lowest value of 2.89983%, as compared to the MDT and Geoid models with these valuesof 5.04123% and 3.02930%, respectively. From the MPE results, it was deduced that the MSSH estimated is off by 2.89983%, the MDT by 5.04123% and the Geoid heightby 3.02930%. Therefore, it can be said that MSSH was estimated with better

accuracy for subsequent years as compared to MDT and Geoid models respectively in the study area.

5.2 Recommendations

In view of the experiences encountered in the course of this study, the following recommendations are made:

i. A reliable Geoid heightmodel for Gulf of Guinea region (Nigeria) can be achieved through multi-mission satellite altimetry technique. Therefore, there is need to integrate oceanography science with geodesy science for an excellent Geoid heightmodel in Nigerian Gulf of Guinea waters.

ii. Since time series analysis reveals that the MSSH may rise from17.9 to 19.2 over the period of 2016 to 2022,research in the field of oceanography should be intensified for proper evaluation to better understand the sea level changes. Consequently, enhance the monitoring and management of the coastal environment.

iii. There is need for the establishment of a network of reliable tidal gauges in Nigerian coastal regions for use in the validation of satellite altimetry data.

5.3 Contribution to Knowledge

The following are the contributions to knowledge from the study:

i. The study modelled the Geoid heightof the sea surface references of the Gulf of Guinea water of Nigeria from Satellite Altimetry Data,

which is useful in the monitoring and management of coastal flooding and erosion.

ii. The study established that a strong relationship exists between the Geoid height, MSSH and MDT.

iii. The study established that MSSH was estimated with better accuracy for subsequent years (2016 to 2022) compared to MDT and Geoid heights respectively over the study area.

REFERENCES

Alexandre, B. L. and Joseph, H. (2012). Use of Recent Geoid Models to Estimate Mean Dynamic Topography And Geostrophic Currents in South Atlantic And Brazil Malvinas Confluence. *Brazilian Journal of Oceanography*, 60(1): (pp. 41-48), 2012.

Andersen, O. B. and Knudsen, P. (2009). DNSC08 mean sea surface and mean dynamic topography models, *J. Geophys. Res*., 114, C11001, doi: 10.1029/2008JC005179.

Anderson, O. B., and Scharroo, R. (2011). Range and geophysical corrections in coastal regions: and implications for mean sea surface determination. In S. Vignudelli, A. Kostianoy, P. Cipollini and J. Benveniste (Eds.), *Coastal Altimetry*, (pp. 103-146). Springer, ISBN 978-3-642-12796-0.

Arora, K. (2011). Geodesy, Figure of the Earth. In Gupta, H., K. (Ed.) *Encyclopedia of Solid Earth Geophysics*. Encyclopedia of Earth Sciences Series. Springer, Dordrecht. doi: 10.1007/978-90-481-8702-7.

AVISO and PODAAC (2008). IGDR and GDR Jason products, edition 4.1, *AVISO SMM-MU-M5-OP-13184-CN, PODAAC JPL D-21352*.,

Baylon, A. M. and Santos, E. M. R., (2013). GIS as an Innovative Tool for Maritime Education Training (MET) Research and Campus Management Enhancement. *Marine Navigation and Safety of Sea Transportation*(pp. 13-22), P.O. Box 11320, 2301 EH Leiden, the Netherlands.CRC Press/Balkema. ISBN: 978-1-315-88315-1

Bosch, W. (2003). Geodetic Application of Satellite Altimetry. In Hwan, C., Shum, C. K., Li, J. (Eds.) Satellite Altimetry for Geodesy, Geophysics and Oceanography,*International Association of Geodesy Symposia*(Vol. 126, pp. 3-21).Verlag: Springer.doi: 10.1007/978-3-642-18861-9_1

Bromirski, D. R. (2008). *Sea Level and Change*, California Energy Commission, 1516 Ninth Street, Sacramento, CA 95814.

Bronner, E., Piccot, N., Desjonqueres, J-D., Desai, S., Hausman, J., Carrer, L., and Tran, N., (2016). *CNES: SALP-MU-M5-OP-13184-CN*. Jason-1 Product, Handbook.

Bruinsnia, S. L., Forste, C., Abrikosov, O., Lemoine, J., Marty, J. Mulet, S., Rio, M. and Bonvalot, S. (2013). ESA's Satellite-only gravity field

model via the direct approach based on all GOCE data. *Geophysical Research Letters*, Vol. 41, Issue 21. doi: 10.102/2014GL062045.

Cartwright, D. E., (1993). Theory of ocean tides with Application to Altimetry. *Satellite Altimetry in Geodesy and Oceanography*, (pp. 99–141), Verlag Berlin Heidelberg:Springer. Retrieved from link.springer.com/chapter/

Central Intelligence Agency, (2005). The CIA World Factbook, 2005, ISSN: 1553-8133. Retrieved from https://b-ok.cc/book/3025175/5a621b.

Chelton, D. B., Ries, J., Haines, B., Fu, L.-L., and Callahan, P., (2001). Satellite altimetry. In Fu, L.-L., and Cazenave, A. (Eds.).*Satellite Altimetry and Earth Sciences*: A Handbook for Techniques and Applications. San Diego. Academic Press, pp. 1–131.

Chidi, O. H. and Ominigbo, O. E. (2010). Climate Change and Coastal Westland: Nigeria in Perspective. *Internatinal Journal of Environmental Issues*, Vol. 7, No. 2: pp 216-223.

Cipollini, P., Benveniste, J. and Vignudelli, S. (2013). Coastal Altimetry Benefits from CryoSat-2 Synthetic Aperture Measurements. *Eos, Transactions American Geophysicall Union*, 94 (8). P81. doi: 10.1002/2013EO080010.

Cipollini, P., Calafat, F., M., Jevrejeva, S., Melet, A. and Prandi, P. (2017). Monitoring SeaLevel in the Coastal Zone with Satellite Altimetry and Tide Gauges. *SurvGeophys*, (2017) 38:33-37. doi: 10.1007/s10712-0169392-57.

DataOne, (2017). Panoply-data-viewer. Retrieved from (www.dataone.org/software-tools/panoply-data-viewer). Accessed 10/05/2017.

Davis, D., Sutherland, M., Jaggan, S. and Singh, D. (2012). Determining and Monitoring Sea Level in the Caribbean using Satellite Altimetry: Knowing to manage the territory, protect the environmentand evaluate the cultural heritage. *FIG Working Week 2012*.

Din, A., H., M., Ses, S., Omar, K., M., Naeije, M.,Yaakob, O. and Pa'suya, M., F. (2014). Derivation of Sea Level Anomaly Based on the Best Range and Geophysical Corrections for Malaysian Seas using Radar Altimeter Database System (RADS). *Journal Teknologi*. doi: 10.11113/jt.v71.3830.

Dorandeu, J., Ablain, M., Le Traon, PY. (2003). Reducing Cross-Track Geoid Gradient Errors around TOPEX/Poseidon and Jason-1 Nominal Tracks: Application to Calculation of Sea Level Anomalies. *Journal of Atmospheric and Oceanic Technology*, Vol. 20 (pp. 1826-1838).

Frappart, F., Papa, F., Famiglietti, F., S., Prigent, C., Rossow, W., B. and Seyler, F. (2008). Interannual Variations of River Water Storage from a Multiple Satellite Approach: A Case Study for the Rio Negro River Basin. *Journal of Geophysical Research*, Vol. 113, D21104. doi: 10.1029/2007JDO9438.

Foreman, M. G. G., Crawford, W. R., Cherniawsky, J. Y., Gower, J. F. R., Guypers, L., and Ballantyne, V. A., (1998). Tidal correction of TOPEX/POSEIDON altimetry for seasonal sea surface elevation and current determination off the Pacific coast of Canada. *Journal of Geophys*, *Res*., 103(C12): 2797927998.

Foreman, M. G. G. and Neufeld, E. T., (1991). Harmonic Tidal Analyses of Long Time Series. *International Hydrographic Review*, Monaco, LXVIII (1).

Fraczek, W. (2003). Mean Sea Level, GPS, and the Geoid. Retrieved from 04-06-2019http://www.esri.com/news/arcuser/0703/geoid1of3.html

Gentry, T. W., Weatherford, L. R. and Wiliamowski, B. M., (2003). Neural Network Forecasting for Airlines: A Csomparative Analysis. *Journal of Revenue and Pricing Management.*Retrievedfrom http://www.researchgate.net/publication/233684273.

Ginzburg, A. I., Kostianoy, A. G., Sheremet, N. A., and Lebedev, S. A. (2010). Introduction and assessment of improved coastal altimetry strategies: Case study over the northwestern Mediterranean Sea.In Vignudelli, S.,Kostianvoy, A., Cipollini, P. and Benveniste, J.(Eds.), *Coastal Altimetry* (pp. 367-388). New York: Springer.

Gomarasca, M. A. (2009). *Basics of Geomatics*, National Research Council of Italy, Institute for the Electromagnetic Sensing of the Environment, Milano, Italy: Springer.

Götze, H.-J. and Li, X. (2001). Ellipsoid, geoid, gravity, geodesy and geophysics: Topography and Geoid Effects on Gravity Anomalies in Mountainous Areas as Inferred from the Gravity Field of the Central Andes. *Phy. Chem. Earth*, Vol. 21, No. 4, pp. 295-297. doi: 10.1190/1.1487109.

Handoko, E. Y., Fernandes, M. J., and Lazaro, C., (2017). Assessment of Altimetric Range and Geophysical Corrections and Mean Sea Surface Models: Impacts on Sea level variability around the Indonesian Seas. *Remote Sensing*, 2017, 9, 102; doi: 10.3390/rs9020102.

Hartanto, P., Huda, S., Putra, W., Variandy, E., D., Triarahmadhana, B., Pangastuti, O., Pahlevi, A., M. and Havang, C. (2018). Estimation of Marine Gravity Anomaly Model from Satellite Altimetry data: Kalimantan and Sulawesi Waters–Indonesia. *Earth and Environmental Science*. doi: 10.1088/1755-1315/162/1/012038

Hermann, D., Alan, H. D., Luiz, P. S. F., Laura, S. and Pedro, S. (2001). Vertical Reference Systems. *International Association of Geodesy symposia*, vol. 124.Verlag Berlin Heidelberg New York: Springer.

Hok, S. F. (2012). Ocean Tides Modeling using Satellite Altimetry. *Geodetic Science*, Report No 501, Ohio State University. Columbus, Ohio 43210.

Hwang, C., Shum, C. K. and Li, J. (Eds.). (2002). Satellite Altimetry for Geodesy, Geophysics and Oceanography. *Proceedings of the International Workshop on Satellite Altimetry*, a joint workshop of lAG Section III Special Study Group SSG3.186 and lAG Section II. Wuhan, China: Springer-Verlag Berlin Heidelberg 2004. doi: 10.1007/978-3-642-18861-9.

IBM SPSS Statistics 25, User Guide, (2018). Retrieved from 06-02-2018,www.ibm.com/support/.

JASON-1 Products Handbook, (2016). Retrieved from 16-10-2017. http://www.class.ncdc.noaa.gov/release/data_available/jason/userhandbook.pdf

Jekeli, C. (2007). Potential Theory and Static Gravity Field of Earth. *Treatise on Geophysics.*doi: 10.1016/B978-0-444-53802-4.00056-7.

Joecila, S., D-S., Frederique, S., Stephane, C., Otto, C., R., F., Emmanuel, R., Afonso, A., M., A. and Jean, L., G. (2010). Water Level Dynamics of Amazon Wetlands at the Watershed Scale by Satellite Altimetry. *International Journal of Remote Sensing*. Taylor and Francis, London. doi: 10.1080/01431161.2010.531914.

Kasenda, A. (2009). High Precision Geoid for Modernization Of Height System In Indonesia. Retrieved from http://unsworks.unsw.edu.au/rep-dis/dpds/rem/unsworks:8446/

Khair, U.,Fahmi, H., Hakim, S. and Rahim, R. (2017). Forecasting Error Calculation with Mean Absolute Deviation and Mean Absolute Percentage Error. *Journal of Physics*: Conference Series, Vol. 930. doi: 10.1088/1742-6596/1/012002.

Kuruk, P., (2004). Customary Water Laws and Practices: Nigeria. Retrieved fromhttp://www.fao.org/legal/advserv/FAOIUCNcs/Nigeria.pdf. Accessed on 06/08/2017.

Lee, H. K., (2008). Radar Altimetry Methods for Solid |Earth Geodynamic Studies. *Geodetic Science and Surveying*, Report No. 489. The Ohio State University Columbus, Ohio 43210.

Le Taron, P. Y., Scheffer, P., Guinehut, S., Rio, M. H., Harnandez, F., Larnicol, G., and Lemoine, J. M. (2001). Mean Ocean Dynamic Topography from GOCE and Altimetry. *CLS Space Oceanography Division*, 8/10 rue Hermes. 31526 Ramonville St. Agne. France.

Li, X., and Hans-Jurgen, Götze. (2002). Ellipsoid, geoid, gravity, geodesy and geophysics. *Geophysics*, Vol. 66, no. 6 (November – December 2001); p.1660–1668, 4 FIGS. doi: 10.1190/1.1487109.

Lisitzin, E., (1974). Sea-Level Changes. *Elsevier Sci. Publ. Co.*, Elsevier Oceanogr. Ser. 8. Amsterdam, Oxford, New York. doi: 10.4319/lo.1975.20.4.0681.

Lyard F., Lefevre F, Letellier, T. and Francis, O. (2006). Modeling the Global Ocean tides: Modern Insights from FES 2004, *Ocean Dynamics*, 56: (pp. 394–415).

Martin, L., Bernadette, M. S., Jens, S. and Nico, S., (2002). Box inverse models, altimetry and the geoid: Problems with the omission error. *Geophysical Research*, Vol. 107, No. C7, 3078, doi: 10.1029/2001JC000855.

Meehl, G. A., Covey, C., Delworth, T., Latif, M., McAveney, B., Mitchell, J. F. B., Stouffer, R. J. and Taylor, K. E. (2007a). Global climate projection: In Climate Change 2007. *The physical Science Basis*, pp 747-846, Cambridge University Press, Cambridge, U. K.

Mimura, N., (2013). Sea-level rise caused by climate change and its implication for society. *The Japan Academy*, 89(7): 281-301. doi:10.2183/pjab.89.281.

Mulet, S., Rio, M. H., and Bruinsma, S. (2012). Assessment of the preliminary GOCE geoid models accuracy for estimating the ocean

mean dynamic topography, Mar. *Geodesy*, 35: 314–336. doi:10.1080/01490419.2012.718230,

Mueller, I. I. (1989). Sea Surface Topography and the Geoid. *Symposium No. 104.*Verlag New York Inc.: Springer.

Niedzielski, T. and Kosek, W. (2009). Forecasting Sea Level Anomalies from TOPEX/Poseidon and Jason-1 satellite altimetry. *Journal of Geodesy*, 83: 469–476.

Ojigi, M. L., Youngu, T. T., Moses, M., Azua, S., Aliyu, Y. A., Sule, J. O. andShebe, M. W. (2016). Mapping of Temporal Variability of Absolute Dynamic Topography in Parts of the Central Atlantic, Using Multi-Mission Satellite Altimetry Data. *Nigeria Journal of Surveying and Geoinformatics*, Vol. 5/1, March, pp. 76-90

Ole, B. A. and Per, K. (2009). DNSC08 mean sea surface and mean dynamic topography models. *Journal of Geophysical Research*, Vol. 114, C11001, doi: 10.1029/2008JC005179.

Onyeka, E. M., and Adaobi, V. M., (2008). Climate Change: A challenge for Environmental Education in the 21st Century. *Multi-disciplinary Journal of Research Development.* 10(5):40-46.

Pail, R., Bruisma, S. L., Migliaccia, F., Förste, C., Goiginger, H., Schuh, W., Hock, E.,Reguzzoni, M., Brockmann, J., Abrikosov, O., Viecherts, M., Fecher, T., Mayrhofer, R. Krasbutter, I., Sansò, F. and Tscherning, C. GOCE gravity field models derived by three different approaches. *Journal of Geodesy,* 85(11): 819-843, doi: 10.1007/s00190-011-0467-x

Paolo, C., Rory, S. and Helen, S., (2013). Product Data Handbook: Coastal Altimetry. *Esurge*. Issue, 1.0, D180A_HB_SL1. In The *Coastal and Marine Research Centre*, University College Cork.

Pattiaratchi, C. (2011). Coastal Tide Guage Observations: Dynamic Processes Present in the Fremantle Record. In: (Ed), *Operational Oceanography in the 21st Century*. Schiller, A. and Brassington, G. B., pp 185-202. doi: 10.1007/978-94-007-0332-2. Springer Dordrecht Heidelberg London New York.

Rajesh, S. &Majumdar, T. J., (2003). Geoid Generation and Sub-surface Structure Delineation under the Bay of Bengal, India Using Satellite Altimeter Data. *Current Sci.*, vol 84, No. 11, pp. 1428-1436.

Ray, R., Egbert, G. D, and Erofeeva, S. Y. (2011). Tide Predictions in Shelf and Coastal Waters: Status and Prospects. In S. Vignudelli, A. G.

Kostianoy, P. Cipollini & J. Benveniste (Eds.), *Coastal Altimetry* (pp. 191-216). Berlin-Springer.

Richard, E. T., William E. (2014). Data Analysis Methods in Physical Oceanography, (3rd Ed.) *Elsevier Science*, ISBN 9780123877826. 225 Wyman Street, Waltham, MA 02451, USA.

Rio, M. H. and Hernandez, F. (2004). A mean dynamic topography computed over the world ocean from altimetry, in situ measurements, and a geoid model. *Journal of geophysical research, vol. 109, c12032,* doi:10.1029/2003jc002226, 2004.

Rio, M. H., Pascual, A., Poulain, P. M., Menna, M., Barceló, B. and Tintoré, J., (2014). Computation of a new mean dynamic topography for the Mediterranean Sea from model outputs, altimeter measurements and oceanographic in situ data. *Ocean Science*, 10, 731-744, 2014. doi: 10.5194/os-10-731-2014.

Sadatipour, S. M. T., Kiamehr, R., Abrehdary, M. and Sharifi, A. R. (2012). The Evaluation of Sea Surface Topography Models based on the Combination of the Satellite altimetry and the Global Geoid Models in the Persian Gulf. *Int. J. Environ. Res., 6(3):* pp. 645-652., ISSN: 1735-6865.

Schaeffer, P., Faugère, Y., Legeais, J. F., Ollivier, A., Guinle, T., and Picot, N. (2012) The CNES_CLS11 Global Mean Sea Surface Computed from, 16 Years of Satellite Altimeter Data, Mar. *Geodesy*, 35, 3–19.

Scott, D. (2002). Sustainable Water Management in the Pacific ISSHAndsAndISSHAnd Vulnerability and Dialogue on Water and Climate. *Pacific Regional Consultation Meeting on Water in Small ISSHAnd Countries,* Sigatoka, Fiji ISSHAnds, 29 July – 3 August 2002, 8.

Scott, D. B. and Medioli, F. S. (2005). Sea Level Indicator – Biological in Depositional Sequences. In M. Schwartz (Ed.) *Encyclopedia of Coastal Science*. Retrieved from http://b-ok.org/book/534126/c515bc/

Seeber, G. (2003). *Satellite Geodesy,* 2nd completely revised and extended edition. Berlin · New York 2003: Walter de Gruyter. doi: 10.1007/978-3-642-28000-9

Sideris, M. G. (2008). Gravity, Geoid and Earth Observation. *International Association of Geodesy Symposia*, Vol. 135.Verlag Berlin Heidelberg: Springer.

Torge, W. (1991). *Geodesy*, Second Edition.Berli. Newyork : Walter de Gruyter. ISBN 3-11-007232-7

UCLOS, (1982). Convention on the Law of the Sea, Dec. 10, 1982, 1833 U.N.T.S. 397.

Unidata, (2012). Structure of NetCDF Files. Retrieved from http://www.unidata.ucar.edu/software/netcdf/workshops/2012), Accessed 15/05/2017

Vameer, M. (2018). Anomalous quantities of the gravity field. *Physical Geodesy Lecture note* pp. 79-116. Retrieved from https://users.aalto.fi/˜mvermeer/fys-.en.pdf

Vignudelli, S., Cipollini, P., Roblou, L., Lyard, F., andGasparini, G. P. (2005). Improved satellite altimetry in coastal systems: Case study of the Corsica Channel (Mediterranean Sea). *Geophysics, Research Letter*, 32: L07608, doi: 10.1029/2005GL022602.

Vignudelli, S., Kostianoy, A. G., and Cipolini, P. (2011). *Coastal Altimetry*,Verlag Berlin Heidelberg: Springer.

Yahaya, N. A. Z., Musa, T. A., Omar, K. M.,Din, A. H. M., Omar, A. H., Tugi, A., and Wahab, M. I. A. (2016). Mean Sea Surface (Mss) Model Determination For Malaysian Seas Using Multi-Mission Satellite Altimeter. *The International Archives of the Photogrammetry, Remote Sensing and Spatial Information Sciences,* Volume XLII-4/W1, 2016.

Xu, G. (2010). *Sciences of Geodesy – I, Advances and Future Directions.* Heidelberg Dordrecht London New York: Springer. Retrieve from http://b-ok.org/book/984580/73773d/

APPENDICES

APPENDIX A: Sampled Datasets from the NetCDF file over the Period of 2008 to 2016

TABLE I

Jul, 2008					
Long (x)	**Lat (y)**	**MSSH**	**MDT**	**SSHA**	**MSSH - MDT**
0	-2	19.223991	0.34527	-0.041225	18.878721
0	-1	18.83905	0.351698	-0.03785	18.487352
3	0	17.849781	0.37032	-0.05215	17.479461
3	1	17.304174	0.381698	-0.037341	16.922476
6	2	16.473442	0.413175	-0.050667	16.060267
6	3	17.479515	0.407933	-0.039792	17.071582
9	4	19.103485	0.422586	-0.004	18.680899
9	5	—	—	—	—
12	6	—	—	—	—

TABLE II

Jul, 2009					
Long (x)	**Lat (y)**	**MSSH**	**MDT**	**SSHA**	**MSSH - MDT**
0	-2	19.225483	0.34539	-0.046175	18.880093
0	-1	18.822275	0.351865	-0.05085	18.47041
3	0	17.827915	0.37067	-0.04295	17.457245
3	1	17.297945	0.381959	-0.025795	16.915986
6	2	16.488092	0.413092	-0.069462	16.075
6	3	17.486509	0.407834	-0.03102	17.078675
9	4	19.085928	0.422486	-0.015	18.663442
9	5	—	—	—	—
12	6	—	—	—	—

TABLE III

Jul, 2010					
Long (x)	Lat (y)	MSSH	MDT	SSHA	MSSH - MDT
0	-2	19.221069	0.345353	-0.054	18.875716
0	-1	18.828899	0.351808	-0.059225	18.477091
3	0	17.838223	0.37053	-0.05515	17.467693
3	1	17.298571	0.381834	-0.049727	16.916737
6	2	16.494316	0.413167	-0.02125	16.081149
6	3	17.503336	0.407826	-0.014	17.09551
9	4	16.494316	0.422429	0.047857	16.071887
9	5	—	—	—	—
12	6	—	—	—	—

TABLE IV

Jul, 2011					
Long (x)	Lat (y)	MSSH	MDT	SSHA	MSSH - MDT
0	-2	19.222591	0.345388	-0.01865	18.877203
0	-1	18.82044	0.351863	-0.025895	18.468577
3	0	17.829517	0.370605	-0.0233	17.458912
3	1	17.308815	0.381844	-0.031535	16.926971
6	2	16.504341	0.413258	-0.02425	16.091083
6	3	17.554348	0.408033	-0.020224	17.146315
9	4	19.01495	0.422383	-0.044667	18.592567
9	5	—	—	—	—
12	6	—	—	—	—

TABLE V

Jul, 2012					
Long (x)	**Lat (y)**	**MSSH**	**MDT**	**SSHA**	**MSSH - MDT**
0	-2	19.222805	0.345305	-0.02895	18.8775
0	-1	18.834393	0.35174	-0.018225	18.482653
3	0	17.817728	0.37083	-0.026425	17.446898
3	1	17.301558	0.381986	-0.029953	16.919572
6	2	16.496782	0.413283	-0.014667	16.083499
6	3	17.535309	0.407631	-0.010939	17.127678
9	4	18.7973	0.4219	-0.017	18.3754
9	5	—	—	—	—
12	6	—	—	—	—

TABLE VI

Jul, 2013					
Long (x)	**Lat (y)**	**MSSH**	**MDT**	**SSHA**	**MSSH - MDT**
0	-2	19.222569	0.345393	-0.055275	18.877176
0	-1	18.821987	0.35188	-0.0564	18.470107
3	0	17.820148	0.370782	-0.051775	17.449366
3	1	17.299889	0.382052	-0.016045	16.917837
6	2	16.473099	0.413208	-0.0165	16.059891
6	3	17.465696	0.4077	-0.019429	17.057996
9	4	19.060667	0.422483	0.059833	18.638184
9	5	—	—	—	—
12	6	—	—	—	—

TABLE VII

Jul, 2014					
Long (x)	**Lat (y)**	**MSSH**	**MDT**	**SSHA**	**MSSH - MDT**
0	-2	19.223755	0.34542	-0.068425	18.878335
0	-1	18.815319	0.351905	-0.073225	18.463414
3	0	17.827398	0.370643	-0.057825	17.456755
3	1	17.309029	0.381865	-0.050163	16.927164
6	2	16.487547	0.413092	-0.042667	16.074455
6	3	17.481413	0.408071	-0.033061	17.073342
9	4	19.024755	0.422414	-0.043286	18.602341
9	5	—	—	—	—
12	6	—	—	—	—

TABLE VIII

Jul, 2015					
Long (x)	**Lat (y)**	**MSSH**	**MDT**	**SSHA**	**MSSH - MDT**
0	-2	19.225294	0.345321	-0.054821	18.879973
0	-1	16.938499	0.35166	-0.0676	16.586839
3	0	17.829174	0.3706	-0.023658	17.458574
3	1	17.304138	0.381959	-0.000167	16.922179
6	2	16.495998	0.413225	-0.01325	16.082773
6	3	17.520128	0.408071	0.01149	17.112057
9	4	19.042982	0.4224	-0.047333	18.620582
9	5	—	—	—	—
12	6	—	—	—	—